

Turbidite Event History—Methods and Implications for Holocene Paleoseismicity of the Cascadia Subduction Zone

Chris Goldfinger¹, C. Hans Nelson², Ann E. Morey¹, Joel E. Johnson¹, Jason R. Patton¹, Eugene Karabanov³, Julia Gutiérrez-Pastor², Andrew T. Eriksson¹, Eulàlia Gràcia⁴, Gita Dunhill⁵, Randolph J. Enkin⁶, Audrey Dallimore⁷, and Tracy Vallier⁸

Abstract

Turbidite systems along the continental margin of Cascadia Basin from Vancouver Island, Canada, to Cape Mendocino, California, United States, have been investigated with swath bathymetry; newly collected and archive piston, gravity, kasten, and box cores; and accelerator mass spectrometry radiocarbon dates. The purpose of this study is to test the applicability of the Holocene turbidite record as a paleoseismic record for the Cascadia subduction zone. The Cascadia Basin is an ideal place to develop a turbidite paleoseismologic method and to record paleoearthquakes because (1) a single subduction-zone fault underlies the Cascadia submarine-canyon systems; (2) multiple tributary canyons and a variety of turbidite systems and sedimentary sources exist to use in tests of synchronous turbidite triggering; (3) the Cascadia trench is completely sediment filled, allowing channel systems to trend seaward across the abyssal plain, rather than merging in the trench; (4) the continental shelf is wide, favoring disconnection of Holocene river systems from their largely Pleistocene canyons; and (5) excellent stratigraphic datums, including the Mazama ash and distinguishable sedimentological and faunal changes near the Pleistocene-Holocene boundary, are present for correlating events and anchoring the temporal framework.

Multiple tributaries to Cascadia Channel with 50- to 150-km spacing, and a wide variety of other turbidite systems with different sedimentary sources contain 13 post-Mazama-ash and 19 Holocene turbidites. Likely correlative sequences are found

in Cascadia Channel, Juan de Fuca Channel off Washington, and Hydrate Ridge slope basin and Astoria Fan off northern and central Oregon. A probable correlative sequence of turbidites is also found in cores on Rogue Apron off southern Oregon. The Hydrate Ridge and Rogue Apron cores also include 12–22 interspersed thinner turbidite beds respectively.

We use ¹⁴C dates, relative-dating tests at channel confluences, and stratigraphic correlation of turbidites to determine whether turbidites deposited in separate channel systems are correlative—triggered by a common event. In most cases, these tests can separate earthquake-triggered turbidity currents from other possible sources. The 10,000-year turbidite record along the Cascadia margin passes several tests for synchronous triggering and correlates well with the shorter onshore paleoseismic record. The synchronicity of a 10,000-year turbidite-event record for 500 km along the northern half of the Cascadia subduction zone is best explained by paleoseismic triggering by great earthquakes. Similarly, we find a likely synchronous record in southern Cascadia, including correlated additional events along the southern margin. We examine the applicability of other regional triggers, such as storm waves, storm surges, hyperpycnal flows, and teletsunami, specifically for the Cascadia margin.

The average age of the oldest turbidite emplacement event in the 10–0-ka series is 9,800±~210 cal yr B.P. and the youngest is 270±~120 cal yr B.P., indistinguishable from the A.D. 1700 (250 cal yr B.P.) Cascadia earthquake. The northern events define a great earthquake recurrence of ~500–530 years. The recurrence times and averages are supported by the thickness of hemipelagic sediment deposited between turbidite beds. The southern Oregon and northern California margins represent at least three segments that include all of the northern ruptures, as well as ~22 thinner turbidites of restricted latitude range that are correlated between multiple sites. At least two northern California sites, Trinidad and Eel Canyon/pools, record additional turbidites, which may be a mix of earthquake and sedimentologically or storm-triggered events, particularly during the early Holocene when a close connection existed between these canyons and associated river systems.

The combined stratigraphic correlations, hemipelagic analysis, and ¹⁴C framework suggest that the Cascadia margin has three rupture modes: (1) 19–20 full-length or nearly

¹ Oregon State University, Corvallis, OR

² Instituto Andaluz de Ciencias de la Tierra, Universidad de Granada, Granada, Spain

³ Institute of Geochemistry, Siberian Branch of Russian Academy of Sciences, Irkutsk, Russia; Chevron Energy Technology Company, Houston, TX

⁴ Centre Mediterrani d'Investigacions Marines i Ambientals Unitat de Tecnologia Marina, Barcelona, Spain

⁵ Department of Earth and Environmental Sciences, California State University, East Bay, Hayward, CA

⁶ Geological Survey of Canada—Pacific, Sydney, B.C., Canada

⁷ Geological Survey of Canada—Pacific, Sydney, B.C., Canada; Royal Roads University, Victoria, B.C., Canada

⁸ U.S. Geological Survey, Menlo Park, CA

2 Turbidite Event History—Methods and Implications for Holocene Paleoseismicity of the Cascadia Subduction Zone

full length ruptures; (2) three or four ruptures comprising the southern 50–70 percent of the margin; and (3) 18–20 smaller southern-margin ruptures during the past 10 k.y., with the possibility of additional southern-margin events that are presently uncorrelated. The shorter rupture extents and thinner turbidites of the southern margin correspond well with spatial extents interpreted from the limited onshore paleoseismic record, supporting margin segmentation of southern Cascadia. The sequence of 41 events defines an average recurrence period for the southern Cascadia margin of ~240 years during the past 10 k.y.

Time-independent probabilities for segmented ruptures range from 7–12 percent in 50 years for full or nearly full margin ruptures to ~21 percent in 50 years for a southern-margin rupture. Time-dependent probabilities are similar for northern margin events at ~7–12 percent and 37–42 percent in 50 years for the southern margin. Failure analysis suggests that by the year 2060, Cascadia will have exceeded ~27 percent of Holocene recurrence intervals for the northern margin and 85 percent of recurrence intervals for the southern margin.

The long earthquake record established in Cascadia allows tests of recurrence models rarely possible elsewhere. Turbidite mass per event along the Cascadia margin reveals a consistent record for many of the Cascadia turbidites. We infer that larger turbidites likely represent larger earthquakes. Mass per event and magnitude estimates also correlate modestly with following time intervals for each event, suggesting that Cascadia full or nearly full margin ruptures weakly support a time-predictable model of recurrence. The long paleoseismic record also suggests a pattern of clustered earthquakes that includes four or five cycles of two to five earthquakes during the past 10 k.y., separated by unusually long intervals.

We suggest that the pattern of long time intervals and longer ruptures for the northern and central margins may be a function of high sediment supply on the incoming plate, smoothing asperities, and potential barriers. The smaller southern Cascadia segments correspond to thinner incoming sediment sections and potentially greater interaction between lower-plate and upper-plate heterogeneities.

The Cascadia Basin turbidite record establishes new paleoseismic techniques utilizing marine turbidite-event stratigraphy during sea-level highstands. These techniques can be applied in other specific settings worldwide, where an extensive fault traverses a continental margin that has several active turbidite systems.

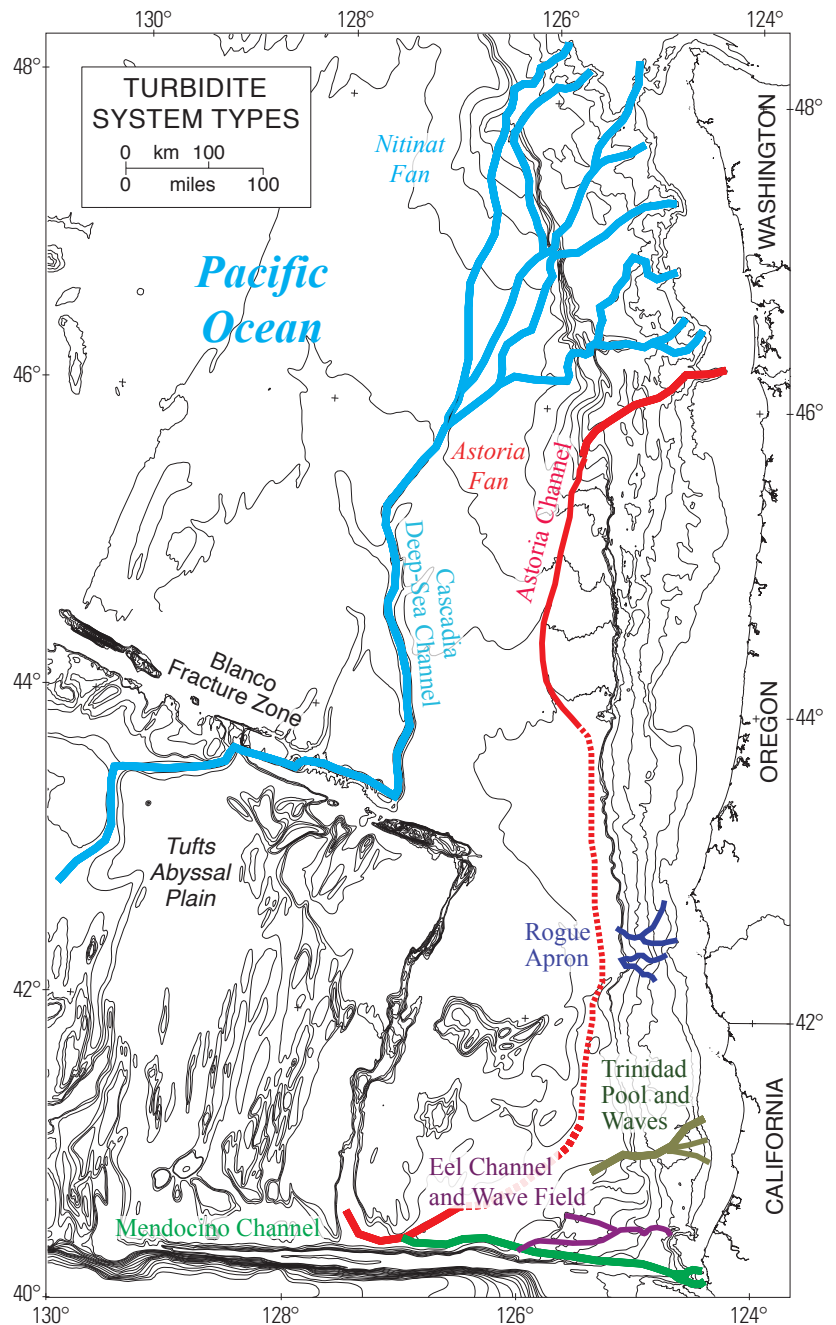


Figure 1. Turbidite-channel and canyon-system types along the Cascadia margin. Dashed portion of Astoria Channel currently has no surface expression, but it is mapped in the subsurface (Wolf and others, 1999).

Introduction

Cascadia Basin includes the deep ocean floor over the Juan de Fuca and Gorda Plates and extends from Vancouver Island, Canada, to the Mendocino Escarpment off northern California, United States (figs. 1, 2). Cascadia Basin contains a variety of Quaternary turbidite systems that exhibit different patterns of channel development and an extensive Holocene

history of turbidite deposition (fig. 1). It has long been known that submarine channels along the Cascadia convergent margin have recorded a Holocene history of turbidites, and recent work suggests that these turbidites are linked to great earthquakes along the Cascadia subduction zone (Adams, 1990; Nelson, C.H., and others, 2000; Goldfinger and others, 2003a,b; Goldfinger and others, 2003a,b, 2008).

Cascadia Basin is an ideal location to examine the linkages between earthquakes and turbidites because the turbidite systems and turbidite history have been studied extensively for the past 40 years, resulting in a large suite of archive cores and associated data and analyses (Duncan, 1968; Duncan and others, 1970; Nelson, C.H., 1968, 1976; Griggs, 1969; Griggs and Kulm, 1970; Carlson and Nelson, 1969). The Holocene stratigraphy of submarine channels along the Cascadia margin includes excellent turbidite marker beds that contain Mazama ash from the eruption of Mount Mazama that formed Crater Lake, Oregon (Nelson, C.H., and others, 1968). The calendar age of the eruption of Mount Mazama has recently been redated at $7,627 \pm 150$ cal yr B.P. from the GISP-2 ice core (Zdanowicz and others, 1999). Airfall from the Mount Mazama eruption was distributed northeastward from southern Oregon, mainly over the Columbia Basin drainage and some of the coastal rivers. It also is found in the Puget lowland, British Columbia (Hallett and others, 1997), and in inlets on the west coast of Vancouver Island (Dallimore and others, 2005b). From these rivers, Mazama ash was transported to temporary depocenters in canyon heads of the Cascadia continental margin, much as Mount St. Helens ash was transported following the 1980 eruption (Nelson, C.H., and others, 1988). Turbidity currents subsequently transported the ash into Cascadia Basin canyon and channel-floor depocenters. The first occurrence of a tuffaceous turbidite dated to the Mount Mazama eruption at each channel site provides a stratigraphic marker to anchor the turbidite sequence and provide opportunities to test for synchronous triggering of turbidity currents for extensive distances along the margin.

We designed our investigation, in part, to test Adams' (1990) hypothesis of a near one-to-one correlation between Holocene great earthquakes and the turbidite-event record in Cascadia Basin channels. Adams observed that 13 post-Mazama turbidites existed at widely separated sites in the Cascadia Basin, that such a coincidence was unlikely, and that the most plausible explanation is that turbidity currents were generated synchronously by subduction-zone earthquakes affecting the entire Cascadia margin. Adams made a convincing case for seismic triggering versus other possible mechanisms, relying on the numerical coincidence and an elegant relative-dating test that established clear synchronicity for part of the margin. Adams used only archive core descriptions, with no age dating or modern sedimentological or stratigraphic techniques. We have tested this hypothesis using new cores collected in 1999 and 2002, accelerator mass spectrometry (AMS) radiocarbon dates, visible and X-ray imagery, and stratigraphic correlation using continuous physical-property measurements to extend the turbidite record in space and time

to the earliest Holocene. During the process, we developed a new turbidite paleoseismic method that tests for synchronicity of turbidite events along strike on convergent and transform margins characterized by single primary faults. Using this method, we evaluate potential triggers of turbidity currents against the time, space, and physical requirements imposed by various mechanisms and develop a paleoseismic record for the Cascadia subduction zone from the turbidite record, where other non-earthquake turbidites can, in many cases, be excluded. Mapping the spatial extent and timing of correlated events can also illustrate segmentation, relative earthquake magnitudes, and spatio-temporal relations that allow testing of recurrence models and stress triggering of margin segments and adjacent fault systems.

We (1) outline the types of turbidite systems found along the Cascadia margin and analyze the channel pathways where the best turbidite event records are preserved; (2) describe the turbidite sequences found in each system; (3) present the radiocarbon, X-ray, computed tomography (CT), visible image, and physical-property data from the core sites; (4) examine the evidence for triggering mechanisms of the Holocene Cascadia turbidites for synchronicity and for stratigraphic correlation of individual events over large distances; (5) present evaluation of the turbidite record as a paleoseismic record for the Cascadia subduction zone; (6) assess the combined onshore and offshore paleoseismic record and propose recurrence intervals and rupture lengths for Holocene great earthquakes in Cascadia; (7) discuss earthquake probabilities and possible recurrence models; and (8) discuss implications of the correlation records for the potential recording of paleoearthquake-source information.

Testing and verification of the turbidite-event paleoseismic technique in Cascadia Basin will help develop fundamental methods that can be applied to other continental-margin systems where an extensive, single, active fault traverses a continental margin that contains several active turbidite systems. Two notable examples are the San Andreas Fault system along the continental margin of northern California (Nelson, C.H., and others, 2000; Goldfinger and others, 2007a, 2008) and the Sunda subduction margin offshore Sumatra (Patton and others, 2007, 2009, 2010).

Significance of Turbidite Paleoseismology

Subduction earthquakes generate some of the largest releases of energy on Earth. Quantifying the mechanisms and patterns of these great events remains elusive, because our observations commonly span only part of a seismic cycle and because the ability to measure the associated strain directly has only recently been developed. Recent rapid advances in Global Positioning System (GPS) technology now make it possible to measure crustal motion associated with elastic-strain accumulation at plate boundaries with a high degree of certainty (for example, McCaffrey and others, 2007; d'Alessio and others, 2005). However, real-time strain measurements

in subduction zones typically represent only a fraction of one strain cycle. Fundamental questions, such as the utility of the seismic-gap hypothesis, clustering, and the applicability of recurrence models, remain largely unanswered because we rarely have a long enough record of earthquake recurrence. Characteristic earthquake models assume that stress buildup is proportional to the time since the last earthquake. The seismic-gap hypothesis follows directly from this assumption and is the basis for probabilistic predictions of seismicity (Nishenko, 1991; Kagan and Jackson, 1995). Characteristic earthquake models and their derivatives have been challenged recently by new models of stress triggering and fault interaction (Stein and others, 1992; Toda and others, 1998; Ward and Goes, 1993; Weldon and others, 2004; Goldfinger and others, 2008). Stress-transfer models have been highly successful where the complex interaction of fault systems can be documented. In these models, strain recharge following an earthquake is supplied only indirectly by the underlying motion of the plates, and the stress on each fault segment is controlled by the action and history of the surrounding segments. What is most needed to address earthquake recurrence and fault interaction is data on spatial and temporal earthquake recurrence for more fault systems over longer spans of time, so that meaningful statistical conclusions may be drawn.

Paleoseismology has the potential to address these questions directly using the geologic record and precise dating during a longer time span than is available to geodesists or seismologists. The use of paleoseismology in active tectonic settings is now advancing rapidly. In the past two decades, discovery of rapidly buried marsh deposits (for example, Atwater and Hemphill-Haley, 1997) and associated tsunami sands (Clague and others, 2000; Kelsey and others, 2005) along the northern Pacific coast of North America, from Vancouver Island to northern California, has led to the recognition that the Cascadia subduction zone, once thought aseismic owing to low instrumental seismicity, likely has generated great (M_w 8–9) earthquakes in the past. The questions of how large and how frequent the megathrust earthquakes are and how these events occur spatially and temporally are now active areas of research in Cascadia and elsewhere (for example, Goldfinger and others, 2008; Nelson, A.R., and others, 2008; Kelsey and others, 2005).

Two avenues for addressing these questions at active continental margins are coastal paleoseismology and investigation of the turbidite-event history. Neither technique uses fault outcrops because the faults are inaccessible, and both techniques must demonstrate that the events they are investigating are generated by earthquakes and not some other natural phenomenon. Nevertheless, these problems can be overcome, and both techniques can be powerful tools for deciphering the earthquake history along an active continental margin (Goldfinger, 2009, 2011a). These methods are complementary; the onshore record provides temporal precision for the most recent events by using radiocarbon dating, coral chronology, and dendrochronology (tree-ring dating), whereas the turbidite record extends farther back in time, at least 10,000 years in

Cascadia, which is long enough to encompass many earthquake cycles. In recent years, turbidite paleoseismology has been attempted in Cascadia (Adams, 1990; Goldfinger and others, 2003a,b, 2008; Nelson, C.H., and others, 1996; Nelson, C.H., and Goldfinger, 1999; Blais-Stevens and Clague, 2001), Puget Sound (Karlin and Abella, 1992; Karlin and others, 2004), Japan (Inouchi and others, 1996), the Mediterranean (Anastasakis and Piper, 1991; Kastens, 1984; Nelson, C.H., and others, 1995b), the Dead Sea (Niemi and Ben-Avraham, 1994), northern California (Field and others, 1982; Field, 1984; Garfield and others, 1994; Goldfinger and others, 2007a, 2008), Lake Lucerne (Schnellmann and others, 2002), Taiwan (Huh and others, 2006), the southwest Iberian margin (Gràcia and others, 2010), the Chile margin (Blumberg and others, 2008; Völker and others, 2008), the Marmara Sea (McHugh and others, 2006; Beck and others, 2007), the Sunda margin (Patton and others, 2007, 2009, 2010), and the Arctic ocean (Grantz and others, 1996). Results from these studies suggest the turbidite paleoseismologic technique is evolving as a useful tool for seismotectonics.

Cascadia Subduction Zone and Great Earthquake Potential

The Cascadia subduction zone is formed by the subduction of the oceanic Juan de Fuca and Gorda Plates beneath the North American Plate off the coast of northern California, Oregon, Washington, and Vancouver Island (fig. 2). The convergence rate is ~35–38 mm/yr directed N. 60° E. at the latitude of Oregon (0.4 m.y. interpolation in Mazotti and others, 2003, depending on models and reference frames). Juan de Fuca-North American convergence is oblique, with obliquity increasing southward along the margin. The submarine forearc widens from 60 km off southern Oregon to 150 km off the northern Olympic Peninsula of Washington, where the thick Pleistocene Astoria and Nitinat Fans presently are being accreted to the margin (fig. 2). The active accretionary thrust faults of the lower slope are characterized by mostly seaward-vergent thrusts on the Oregon margin from lat 42° N. to lat 44°55' N. and north of lat 48°08' N. off Vancouver Island and by landward-vergent thrusts between lat 44°55' N. and lat 48°08' N., on the northern Oregon and Washington margins. The landward-vergent province of the northern Oregon and Washington lower slope may be related to subduction of rapidly deposited and overpressured sediment from the Nitinat and Astoria Fans (Seely, 1977; MacKay, 1995; Goldfinger and others, 1997; Adam and others, 2004). Off Washington and northern Oregon, the broad accretionary prism is characterized by a low wedge taper and widely spaced landward-vergent accretionary thrusts and folds (which scrape off virtually all of the incoming sedimentary section). Sparse age data suggest that this prism is Quaternary in age and is building westward at a rate similar to the orthogonal component of plate convergence (Westbrook, 1994; Goldfinger and others, 1996). This young wedge abuts a steep slope break that separates it from

the continental shelf. Much of onshore western Oregon and Washington and the continental shelf of Oregon is underlain by a basement of Paleocene to middle Eocene oceanic basalt with interbedded sediments known as the Crescent or Siletzia terrane. This terrane may have been accreted to the margin (Duncan, 1982) or formed by in-situ rifting and extension parallel to the margin (for example, Wells and others, 1984). Much of the Oregon and Washington shelf is underlain by a moderately deformed Eocene through Holocene forearc-basin sequence.

The earthquake potential of Cascadia has been the subject of major paradigm changes in recent years. First thought to be aseismic owing to the lack of historical seismicity, great thickness of subducted sediments, and low uplift rates of marine terraces (Ando and Balazs, 1979; West and McCrumb, 1988), Cascadia is now thought capable of producing great subduction earthquakes on the basis of paleoseismic and tsunami evidence (for example, Atwater, 1987; Atwater and others, 1995; Darienzo and Peterson, 1990; Nelson, A.R., and others, 1995; Satake and others, 1996, 2003), geodetic evidence of elastic strain accumulation (for example, Mitchell and others, 1994; Savage and Lisowski, 1991; Hyndman and Wang, 1995; Mazotti and others, 2003; McCaffrey and others, 2000), and comparisons with other subduction zones (for example, Atwater, 1987; Heaton and Kanamori, 1984). Despite the presence of abundant paleoseismic evidence for rapid coastal subsidence and tsunamis, the Cascadia plate boundary remains the quietest of all subduction zones, with only one significant interplate thrust event ever recorded instrumentally (Oppenheimer and others, 1993). Cascadia represents an end member of the world's subduction zones in both seismic activity (Acharya, 1992) and temperature. The Cascadia plate interface is among the hottest subduction thrusts, because of its young subducting lithosphere and thick blanket of insulating sediments (McCaffrey, 1997).

With the past occurrence of great earthquakes in Cascadia now well established, attention has turned to magnitude, recurrence intervals, and segmentation of the margin. Geodetic leveling surveys across the onshore Cascadia forearc show that some areas are tilting landward on a time scale of 70 years. These data indicate that tilting is occurring parallel to the arc. Mitchell and others (1994) calculated tectonic uplift rates from the leveling data using ties to tide gauges. The uplift signal is highly variable along strike in Cascadia; central Oregon and central Washington are apparently undergoing no tectonic uplift, whereas other areas are rising at rates of 1–4 mm/yr. The geodetic uplift rates in the fast-rising areas greatly exceed the geologically determined rates of marine-terrace uplift and have thus been attributed to elastic-strain accumulation preceding a future subduction zone earthquake (Mitchell and others, 1994; Hyndman and Wang, 1995; Burgette and others, 2009). Elastic-dislocation models based on thermal and GPS data indicate that the locked plate boundary must lie offshore (Hyndman and Wang, 1995; Mitchell and others, 1994; McCaffrey and others, 2000, 2007); however, the meaning and existence of the high variability in rates is controversial.

Hyndman and Wang (1995) attribute the variability to artifacts in data processing, whereas Mitchell and others (1994) consider them the real products of a locked zone of varying width. Goldfinger and McNeill (2006) and Priest and others (2009) suggest that structural evidence offshore supports long-term asperities underlying uplifted submarine structural highs offshore that coincide with areas of rapid uplift onshore. In contrast, Wells and others (2003) proposed a forearc-basin-centered asperity model for Cascadia and elsewhere. Recent evidence of episodic tremor and slip (ETS) events down-dip of the locked interface (Brudzinski and Allen, 2007) also may reveal evidence of segmentation. The significance of the debate about the configuration of the Cascadia locked zone is that there may or may not be seismic segments controlled by the thermal or structural boundaries and which, thus, control slip distribution and tsunami generation. Segmented- and whole-margin ruptures should leave distinctly different stratigraphic records in both the coastal marshes and the offshore turbidite-channel systems, which we discuss below.

Methods

Bathymetric Analysis of Turbidite Pathways and Core Siting

Before our 1999 cruise, we integrated all available swath bathymetry and archive core datasets from Cascadia Basin into a geographic information system (GIS) database for channel-pathway analysis that included physiography, axial gradients, and slope-stability/slumping assessments. We included numerous seismic-reflection profiles that were used to evaluate turbidite pathways and recency of activity from Wolf and others (1999). During the *R/V Melville* cruise (1999) and three prior cruises, we collected ~9,000 km² of new multibeam data off the Vancouver Island, Washington, Oregon, and northern California margins using the SeaBeam 2000, SeaBeam Classic, and Hydrosweep systems. Data were edited and corrected for water velocity using velocity profiles calculated from temperature data collected using daily expendable bathythermograph (XBT) casts. Integration of the Washington data presented considerable difficulty because no publicly available multibeam data existed. Not having adequate ship time to survey the entire Washington margin, we found that combining the new multibeam data with sparse soundings was inadequate to define modern sediment-transport pathways clearly. We have attempted to better define these pathways by developing a new bathymetric grid for the Washington continental slope. The grid was composed of areas with and without modern multibeam data. For areas without multibeam data, we hand-contoured the existing soundings in a GIS, while using the GLORIA regional sidescan dataset (EEZScan-84, 1986) to define the detailed morphology of the accretionary prism. This allowed us to interpret the map pattern of canyons, anticlines, and synclines in considerable detail, while honoring the height

Although other mechanisms certainly exist, each is problematic in terms of triggering competence, frequency, synchronicity, or the sustainability of transport of sand-size material to the abyssal plain. During great earthquakes, on the other hand, the entire canyon system is affected, a length of the canyon that can exceed 100 km in Cascadia. The rupture zone also underlies the full length of all of the Cascadia canyons at a shallow depth, making a near ideal setting for causing slope failures. During a great earthquake, the hypocentral distance to a locked fault is never more than 2–10 km from the canyon walls (slab model of McCrory and others, 2006), which likely fail in nearly continuous wall failure during the severe ground shaking of a large earthquake. Peak ground accelerations at such short hypocentral distances are unknown, but can be estimated using the attenuation relations of Atkinson and Boore (1997) and Youngs and others (1997). Using a source-to-site distance of 10 km and $M_w = 9.0$, spectral acceleration can approach 2 g (Youngs and others, 1997, soil site) or 3.5 g (Atkinson and Boore, 1997, rock site only). This represents a tremendous suspension and liquefaction force far greater than anything possible from surface waves and has been recently confirmed by the March 11, 2011, Tohoku earthquake, in which ground acceleration along the coast exceeded 2.7 g as much as 75 km from the fault (<http://nsmpr.wr.usgs.gov/ekalkan/Tohoku/index.html>).

Another key piece of evidence that can be used to address multiple triggering mechanisms is the data from Hydrate Ridge. As previously noted, the Hydrate Ridge west basin is completely isolated from land and shallow water sources of sedimentation. It is a lower slope basin at a depth of ~2,275 m, and the only sediment source is the western flank of Hydrate Ridge, a seaward-vergent anticline. The ridge rises 1,800 m above the basin floor, and the basin is guarded on all sides by structural ridges that prevent downslope transport into the basin from any source other than the flanks of the ridge itself. The surrounding ridges are 500 m high on the north, 1,800 m on the east, and 1,200 m on the south (fig. 29). The west side is bounded by a low sill. The direct downslope transport path to the core sites is clearly visible in the high-resolution deep-towed sidescan-sonar data presented by Johnson and others (2004). The physiography and great depth of the basin eliminate input from storms, tsunami, hyperpycnal flow, and other external sources, as evidenced by the absence of Mazama ash at Hydrate Ridge. There are also no large rivers along the central Oregon coast and no canyon systems between Astoria Canyon (lat 46° N.) and Rogue Canyon (lat 42.2° N.), a distance of 420 km.

Given the exclusion of river, tsunami, or storm-derived material, Hydrate Ridge acts as a control site, limiting the number of potential triggers for turbidity currents to earthquakes (both regional and local), gas hydrate destabilization, and sediment self-failure. The turbidite record at Hydrate Ridge, however, closely matches that of the nearest core sites at Rogue Apron. Stratigraphic correlation between these two sites is good, and ^{14}C age matches also are good, with some exceptions (fig. 45). The turbidite records at these two sites both contain large events (T14 is very subdued at Hydrate Ridge), most of which are close stratigraphic (physical-property trace) matches. We infer that the close stratigraphic

correlation, permissive ^{14}C data, and the identical number of large events in the Hydrate Ridge cores make nonregional earthquake sources unlikely, with the possible exception of one uncorrelated event observed in the most proximal core (fig. 30).

Finally, the recurrence intervals of Cascadia Basin offshore turbidites (Trinidad, Eel, and Mendocino systems excepted) closely match that of the onshore paleoseismic record where temporal overlap exists (Goldfinger and others, 2003a, 2007a, 2008), further discussed in the following section. From the preceding discussion, we conclude that great earthquakes are the best explanation for the observed turbidite record in Cascadia Basin and that uncorrelated turbidites are few. Within this constrained dataset, in the following sections, we discuss the marine turbidite and onshore paleoseismic record and the implications of a long-term earthquake history along the Cascadia margin.

Cascadia Paleoseismic Record

Given the strong evidence for earthquake triggering of the Cascadia marine-turbidite record, with the exceptions discussed previously, we examine the results of this record in terms of the temporal history and margin segmentation of Cascadia paleoearthquakes. The turbidite record in each channel system is summarized in figure 51, and the event time series is given in table 10. Table 10 gives averaged ages for events we interpret as correlative, as well as 2σ -rms error ranges, constrained ages, and 2σ ranges combined and modeled with OxCal. OxCal output is shown in appendix 8, and OxCal input code is included as appendix 9. Because the extensive onshore paleoseismic record exists and provides a strong complimentary dataset for the late Holocene, we first discuss the potential for integration of the onshore and marine paleoseismic records.

Integrating the Onshore and Marine Paleoseismic Records

Coseismic subsidence in the last few thousand years has been well documented in coastal bays and estuaries in the form of rapidly subsided marsh deposits and tsunami sand sheets along the Cascadia coastline (for example, Atwater, 1987, 1992; Clague and Bobrowsky, 1994a,b; Williams and others, 2005; Darienzo and Peterson, 1990; Atwater and others, 1995; Nelson, A.R., and others, 1995, 2006, 2008; Kelsey and others, 2005; Witter and others, 2003). These events indicate sudden coseismic submergence, inundation of coastal lowlands, and burial of the former land surface. Subsidence results from the sudden elastic rebound of the land surface during the earthquake, following gradual uplift during the interseismic period, but the sign of the motion at the coast differs in different subduction zones. Such elastic rebound of land surfaces also has been documented following the 1960 Chilean and 1964 Alaskan subduction earthquakes (Plafker, 1969, 1972). Coastal evidence also includes tsunami runup or washover deposits of thin marine-sand layers with diatoms that are interbedded within estuarine or lake muds (Hemphill-Haley, 1995; Hutchinson and others, 2000; Kelsey and others, 2005; Nelson, A.R., and others, 2006). The tsunami deposits are found several kilometers inland from the coast up river estuaries or in low-lying freshwater lakes near sea level, but above the reach of storm surges. A ~3,500-yr

record of such tsunami events is found in Willapa Bay, Washington (Atwater and Hemphill-Haley, 1997). A 7,300-yr record of lake disturbances is found in Bradley Lake, Oregon (Kelsey and others, 2005). A 5,500-yr record is found in Sixes River estuary, Oregon (Kelsey and others, 1998, 2002). Similar evidence has been found at virtually all bays and estuaries along the Cascadia margin.

Correlation of coseismic subsidence events from site to site is dependent on age control with sufficient precision to distinguish between separate events. Recently, AMS and high-precision radiocarbon and dendrochronology dates for several sites have significantly reduced errors to ± 10 – 20 years or less (Nelson, A.R., and others, 1995; B. Atwater, oral commun., 1997), but suitable material is often unavailable or is stratigraphically positioned above or below the event of interest. The most abundant high-precision data are available for the most recent subsidence event, which probably occurred within a few decades of A.D. 1700, ~ 311 years ago. Dendrochronology of western red cedar in Washington and in northern Oregon estuaries shows death occurred between summer A.D. 1699 and spring A.D. 1700 (Jacoby and others, 1997; Yamaguchi and others, 1997), and less precise dates bracket these dates. The age of this event is supported by evidence of a far-field tsunami in Japan on January 26, A.D. 1700, which has been attributed to a subduction earthquake on the Cascadia subduction zone (Satake and others, 1996, 2003). The A.D. 1700 event is widespread, with evidence found from northern California to Vancouver Island. For older events, error bars for numerical dates are significantly larger, and the difficulty in identifying anomalous local subsidence events increases.

We have compiled all published and available land paleoseismic data in appendix 10. To compare the extensive onshore data with the marine record, we summarize both datasets in figure 52A–C and refer the reader to compilations of both in appendixes 1 and 10. This figure shows the spatial and temporal Holocene earthquake data and our interpreted relations between coastal and marine sites.

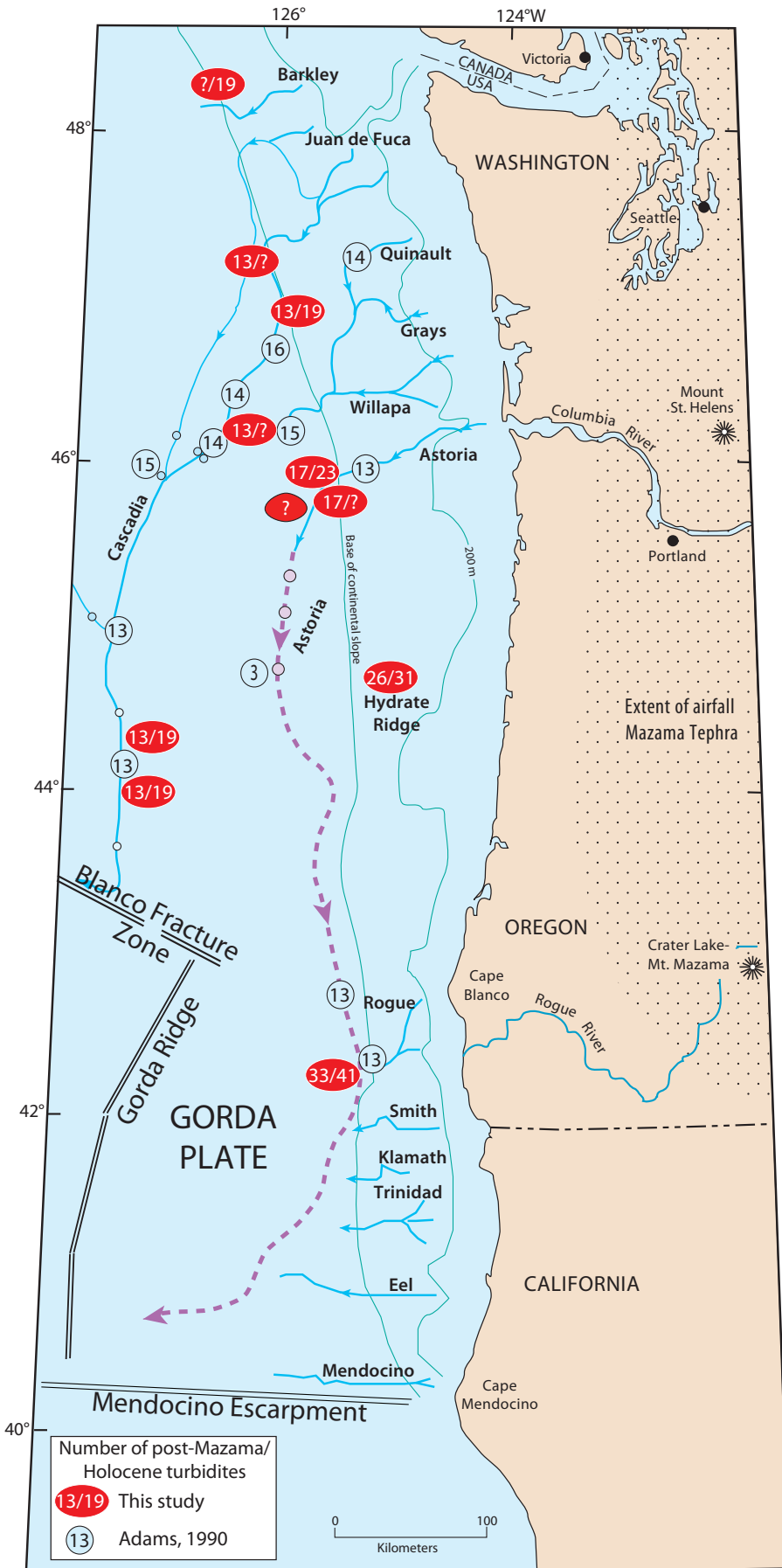
The onshore events have been investigated during a period of more than 25 years, and techniques have evolved considerably in that time. Details of the tests applied to individual sites to test for earthquake origin also vary and are contained in the original literature. Early studies tended to use bulk peat samples from below and sometimes above the tsunami or subsidence-event deposits, with conventional

Table 10. Turbidite age averages and OxCal “combines” and 2σ ranges, Cascadia subduction zone.

Turbidite age averages and OxCal “combines” and $2s$ ranges, Cascadia subduction one.

Event number	Mean turbidite age, in years	RMS 2σ +	RMS 2σ -	Standard deviation	OxCal combined event ages, in years		
T1	265	106	126	11	268	339	200
T2	481	92	97	83	494	548	448
T2a	548	114	122	Single age	601	728	466
T3	796	109	117	55	801	840	760
T3a	1,066	110	123	4	1,076	1,211	947
T4	1,243	105	124	42	1,228	1,278	1,178
T4a	1,422	126	137	84	1,386	1,520	1,246
T5	1,554	177	170	32	1,578	1,650	1,510
T5a	1,820	169	158	61	1,853	1,997	1,721
T5b	2,040	158	157	28	2,071	2,244	1,889
T5c	2,317	139	149	Single age	2,294	2,493	2,087
T6	2,536	137	147	22	2,563	2,617	2,506
T6a	2,730	139	149	Single age	2,767	3,059	2,483
T6b	2,822	143	171	Single age	2,825	3,119	2,529
T7	3,028	134	163	61	3,041	3,127	2,951
T7a	3,157	136	165	Single age	3,182	3,481	2,881
T8	3,443	153	156	68	3,473	3,553	3,392
T8a	3,599	156	159	Single age	3,613	3,958	3,274
T8b	3,890	173	193	Single age	3,891	4,265	3,521
T9	4,108	170	190	52	4,111	4,187	4,038
T9a	4,438	160	168	115	4,498	4,634	4,376
T9b	4,535	174	194	Single age	4,533	4,789	4,266
T10	4,770	170	191	51	4,761	4,864	4,666
T10a	5,062	258	291	16	5,050	5,223	4,884
T10b (T10R1)	5,260	148	201	38	5,273	5,342	5,202
T10c	5,390	152	204	Single age	5,389	5,671	5,107
T10d	5,735	146	143	Single age	5,769	6,059	5,480
T10e	Undated	0	0	0			
T10f (T10R2)	5,772	141	138	106	5,808	6,007	5,609
T11	5,959	141	135	111	5,893	5,989	5,796
T12	6,466	146	133	102	6,445	6,542	6,348
T12a	6,903	127	125	Single age	6,877	7,125	6,625
T13	7,182	122	120	44	7,169	7,217	7,121
T14	7,625	138	138	39	7,608	7,668	7,547
T14a	7,943	141	141	Single age	7,946	8,229	7,665
T15	8,173	183	135	95	8,181	8,292	8,070
T15a	8,459	187	139	Single age	8,449	8,780	8,123
T16	8,906	160	145	62	8,936	9,103	8,775
T16a	9,074	166	151	Single age	9,055	9,374	8,744
T17	9,101	259	291	38	9,088	9,215	8,962
T17a	9,218	211	229	39	9,192	9,355	8,997
T18	9,795	184	232	94	9,758	9,913	9,629

^{14}C dates (for example, Peterson and Darienzo, 1996). As techniques evolved, close maximum or close minimum dates were determined through more careful selection of individual rhizomes or seeds, needles, and twigs close to the event interface, and dating was done using AMS radiocarbon techniques (for example, Nelson, A.R., and others, 2008). Most dates reported were close maximums (dated underneath the events), and thus, like the marine dates, are likely biased somewhat older than the event age (for example, Nelson, A.R., and others, 2008). We favor the most recent work in which origin tests and sampling methods are more robust than in the earlier works; and we favor sites that have multiple well-constrained dates for each event and dates that use seeds and needles over those that use peat and detrital plant



material. Event records vary somewhat in their preservation of events and in natural variability that comes from segmented margin ruptures. In figure 52 and the following discussion, we present our preferred correlation between coastal and marine paleoseismic records and discuss in detail the issues that arise from such comparisons, with emphasis on the discrepancies. These data also are found in the Land-Marine compilation section of appendix 1. For the most part, the onshore data are presented as published, with several exceptions. In cases where single preferred dates were available in ^{14}C years, we recalibrated these data using Calib 5.0.2 both for consistency and to extract the PDF information. Where these data were unavailable or where published data were combinations of multiple dates from OxCal, but PDF information was unavailable, we use the midpoint of the 2σ range for plotting purposes in figure 52.

The differences between dates at onshore sites are great enough in many cases that many onshore events cannot be correlated reliably on the basis of ^{14}C dates, a proposition that is problematic even with much more precise data (for example, Biasi and others, 2002; Schärer and others, 2007). Event 3, for example, is discussed as a possible segmented event by Nelson, A.R., and others (2008) because of this age disparity, whereas offshore, the stratigraphic correlation and tighter age spread suggest it was most likely a single marginwide event. Alternatively, there could be two events, closely spaced in time, that the marine record does not resolve. A similar situation exists along the northern margin with a number of sites reporting a tsunami and earthquake subsidence around 2,000 cal yr B.P., a time for which no marine correlative is found offshore and for which we have no explanation. The space-time diagram of figure 52 relies primarily on the marine record, using stratigraphic correlation to address a number of lesser disparities that radiocarbon dating cannot resolve. Here we discuss primarily the notable unresolved conflicts between the datasets.

Figure 51. Summary of the number of observed post-Mazama and Holocene turbidites in Cascadia Basin turbidite systems from this study and archive cores of Duncan (1968), Griggs (1969), and Nelson, C.H., (1968) that were used in Adams (1990) compilation.

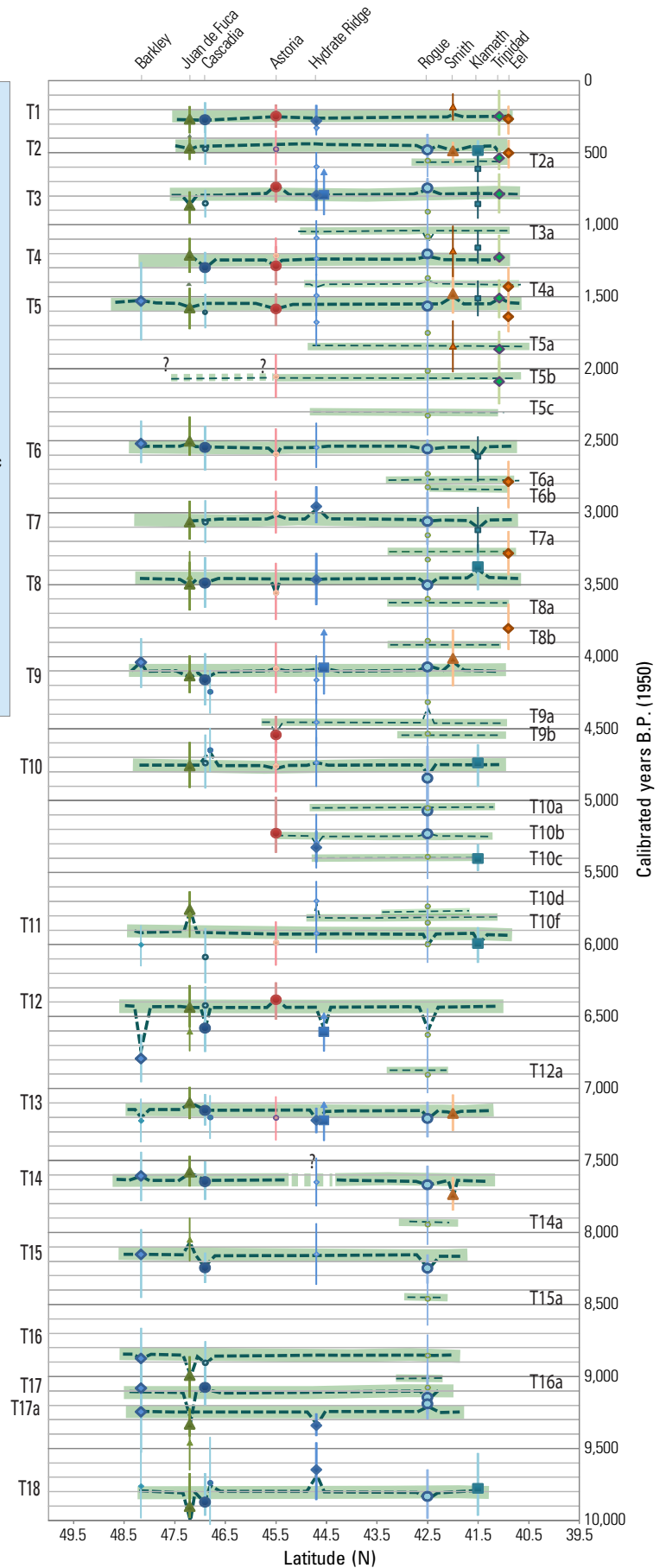
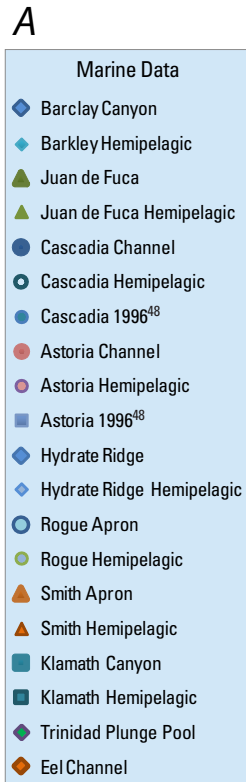


Figure 52. *A*, Space-time diagram for the Cascadia margin showing Holocene marine radiocarbon data and stratigraphic correlations. Filled symbols are marine ¹⁴C ages, smaller filled symbols are hemipelagic calculated ages. Marine data are plotted as 2σ midpoints and 2σ ranges. Plotted ages correspond to the land-marine compilation tab in appendix 1. Dashed lines show stratigraphic correlation of the turbidite data, which show deviations from the preferred age range where correlation overrules an individual ¹⁴C age. Up arrows are shown for marine data where sitewide erosion suggests a maximum age. Marine error ranges are 2σ-rms propagated errors. Smaller southern Cascadia events are indicated with thinner dashed lines. Green bars are best fitting offshore-onshore age trends for Cascadia earthquakes. *B*, As in *A*, with high-precision land data added. Land data are plotted as published, with some sites revised as discussed in text. Preference among land sites is given to recent publications that use well-constrained ages. Down arrows indicate minimum ages as published (land only). Two-sided arrows are shown where maximum and minimum ages are averaged (land sites only). *C*, As in *B*, with additional lower precision land data, including early bulk peat ages. Superscript numerals in the legend are keyed to publications cited in the References tab of appendix 1 (marine data) and appendix 10 (terrestrial data). Marine ¹⁴C data are given in appendix 1; onshore data are given in appendix 11.

Figure 52. *A*, Space-time diagram for the Cascadia margin showing Holocene marine radiocarbon data and stratigraphic correlations. Filled symbols are marine ¹⁴C ages, smaller filled symbols are hemipelagic calculated ages. Marine data are plotted as 2σ midpoints and 2σ ranges. Plotted ages correspond to the land-marine compilation tab in appendix 1. Dashed lines show stratigraphic correlation of the turbidite data, which show deviations from the preferred age range where correlation overrules an individual ¹⁴C age. Up arrows are shown for marine data where sitewide erosion suggests a maximum age. Marine error ranges are 2σ-rms propagated errors. Smaller southern Cascadia events are indicated with thinner dashed lines. Green bars are best fitting offshore-onshore age trends for Cascadia earthquakes. *B*, As in *A*, with high-precision land data added. Land data are plotted as published, with some sites revised as discussed in text. Preference among land sites is given to recent publications that use well-constrained ages. Down arrows indicate minimum ages as published (land only). Two-sided arrows are shown where maximum and minimum ages are averaged (land sites only). *C*, As in *B*, with additional lower precision land data, including early bulk peat ages. Superscript numerals in the legend are keyed to publications cited in the References tab of appendix 1 (marine data) and appendix 10 (terrestrial data). Marine ¹⁴C data are given in appendix 1; onshore data are given in appendix 11—continued.

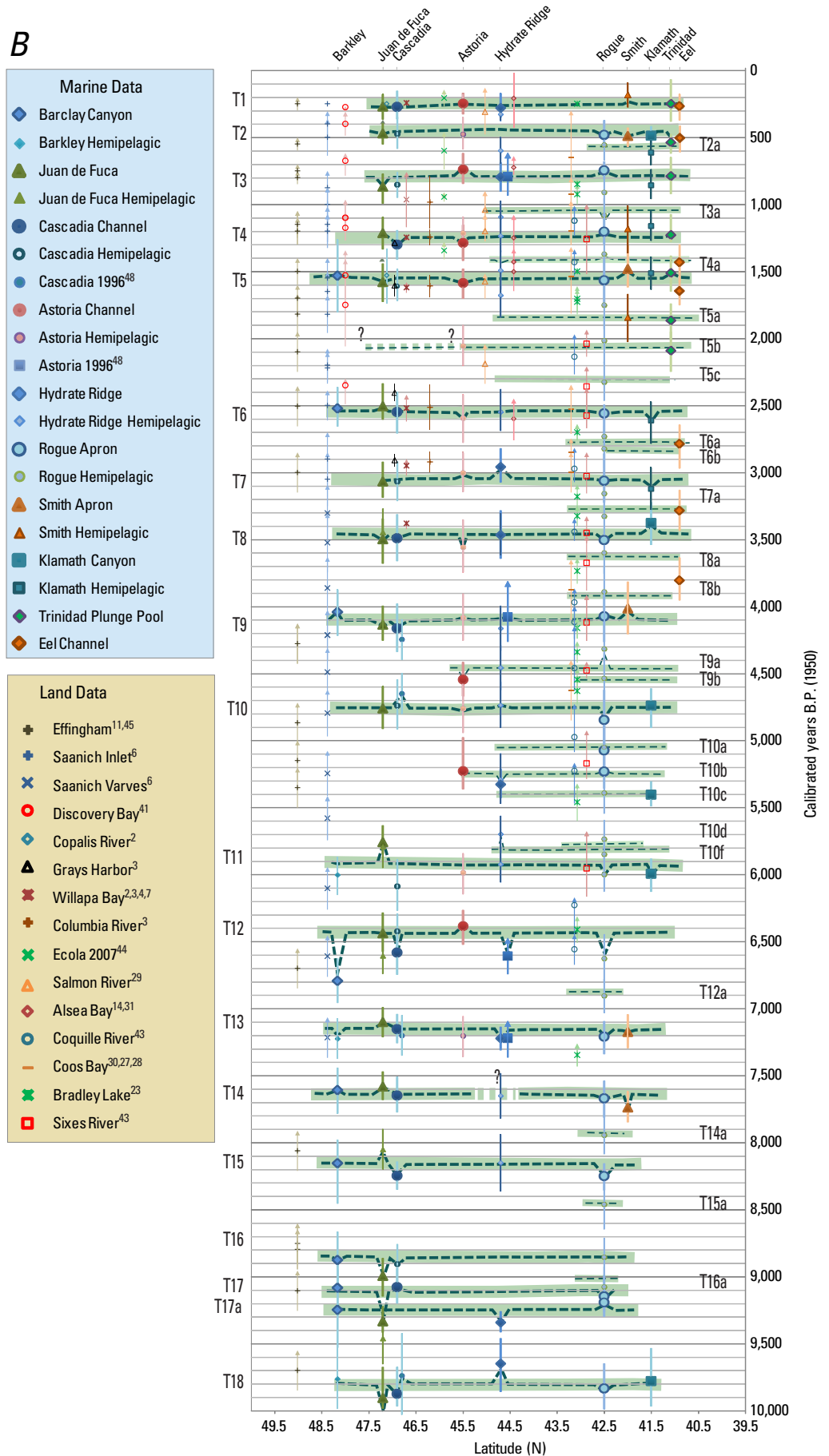
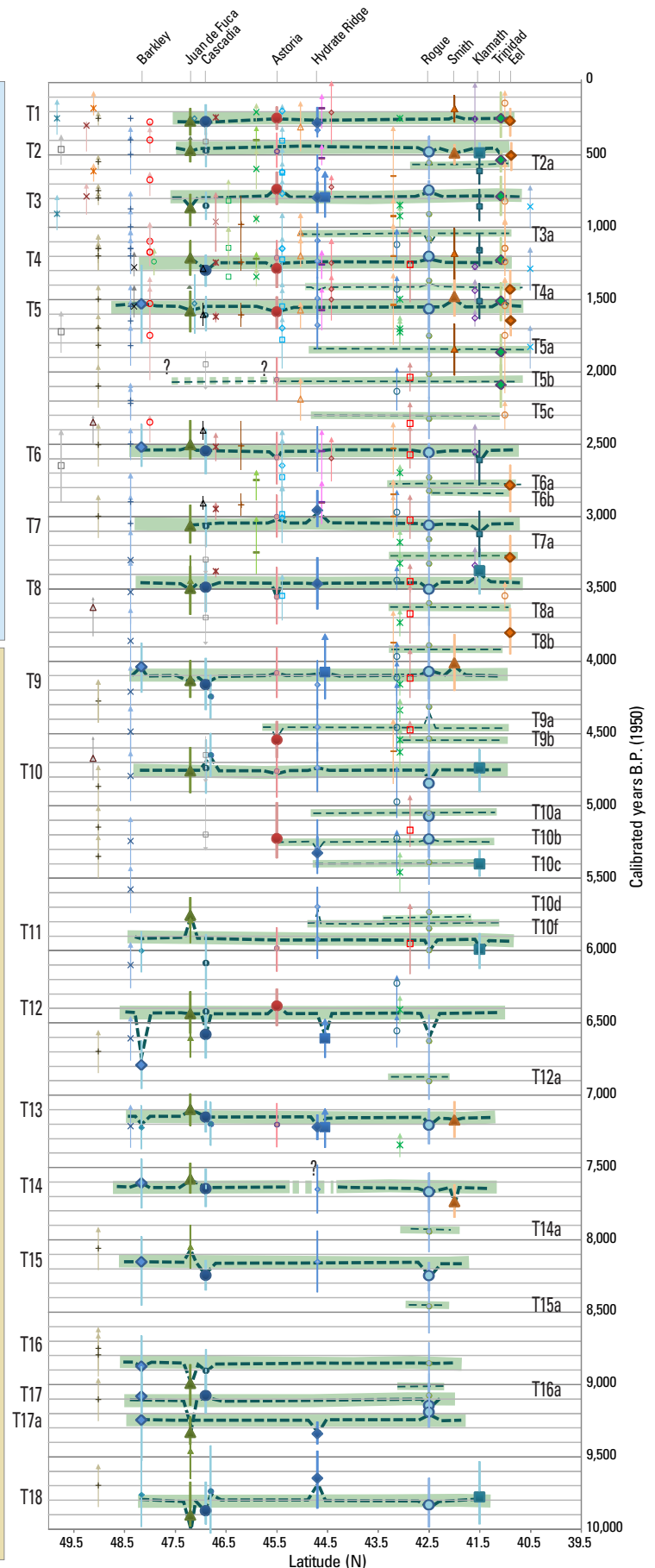


Figure 52. *A*, Space-time diagram for the Cascadia margin showing Holocene marine radiocarbon data and stratigraphic correlations. Filled symbols are marine ¹⁴C ages, smaller filled symbols are hemipelagic calculated ages. Marine data are plotted as 2σ midpoints and 2σ ranges. Plotted ages correspond to the land-marine compilation tab in appendix 1. Dashed lines show stratigraphic correlation of the turbidite data, which show deviations from the preferred age range where correlation overrules an individual ¹⁴C age. Up arrows are shown for marine data where sitewide erosion suggests a maximum age. Marine error ranges are 2σ-rms propagated errors. Smaller southern Cascadia events are indicated with thinner dashed lines. Green bars are best fitting offshore-onshore age trends for Cascadia earthquakes. *B*, As in *A*, with high-precision land data added. Land data are plotted as published, with some sites revised as discussed in text. Preference among land sites is given to recent publications that use well-constrained ages. Down arrows indicate minimum ages as published (land only). Two-sided arrows are shown where maximum and minimum ages are averaged (land sites only). *C*, As in *B*, with additional lower precision land data, including early bulk peat ages. Superscript numerals in the legend are keyed to publications cited in the References tab of appendix 1 (marine data) and appendix 10 (terrestrial data). Marine ¹⁴C data are given in appendix 1; onshore data are given in appendix 11—continued.



We observe some systematic age differences between coastal and marine age sequences that otherwise appear likely to represent correlatable events. The basis for this statement is that both datasets have passed independent tests of earthquake origin, and thus the chances of having separate earthquake sequences, one recorded onshore but not offshore, and vice versa, must be considered very low. Offshore dates can be biased in time by unmodeled marine-reservoir variability, which we suspect may account for some age disparities. Onshore dates also may be biased in time, including offsets from dating of detrital material and contamination from younger material, such as roots from a higher stratigraphic level. In several cases, the variability does not appear systematic and may simply be scatter owing to unidentified errors. In cases of clear systematics, we use these differences to model temporal and spatial reservoir variability, along with the difference in benthic and planktic foraminiferal dates, as discussed previously.

For a given time range where overlap exists and a given latitude range, the total number of events, whether onshore or offshore, is similar, with a few differences noted below. The nearly identical recurrence values support our inference that both records are most likely recording the same earthquake series. We suggest that the thinner, spatially limited turbidites offshore are, in many cases, the same events recorded at the more sensitive sites onshore, such as Bradley Lake. Considering the offshore record alone, these turbidites do not have the benefit of the same variety of synchronicity tests that the marginwide events do.

Some of the smallest turbidites offshore appear to be represented by spotty or no record onshore. Although this reduces our confidence in these events to some degree, it is consistent with a reasonable scenario in which smaller earthquakes would be expected to leave a more discontinuous geologic record onshore and offshore. For example, potential correlatives for marine event T2 are observed at many but not all onshore sites (Tofino, Ucluelet, Johns River, Discovery Bay, Netarts Bay, and Ecola Creek; see fig. 2). Where coseismic subsidence data are available for this earthquake, they suggest minimal subsidence relative to other events (Shennan and others, 1998). We also note that the smaller turbidites of limited latitudinal extent correspond reasonably well in age to the local southern Oregon events, where they have been dated or their approximate ages calculated. These earthquakes have limited rupture length in both onshore and offshore records, suggesting a first-order compatibility between offshore turbidite size, shaking intensity or duration (controlling turbidite mass) and rupture length. The offshore rupture limits discussed in subsequent sections are derived from our interpretation of the combined coastal/marine data shown in figure 52.

Discovery Bay

In a few cases, dated events onshore were interpreted as upper plate earthquakes because they did not appear in the existing coastal paleoseismic record (events 2 and 3 in Discovery Bay; Williams and others, 2005). However, these events are included in figure 52 because the original interpretations

were based on the interpreted fit, or lack thereof, to existing paleoseismic data, rather than any independent metric of origin. Some of these events appear nonetheless to be a reasonable fit to the Cascadia earthquake time series offshore, which seems to better capture smaller earthquakes than the onshore paleoseismic sites. Resolution of such discrepancies is beyond the scope of this report and will require further research.

Willapa Bay, Grays Harbor, Columbia River, Southwest Washington and Northern Oregon

One of the best documented land paleoseismic sites is the Willapa Bay, Wash., area (Atwater and Hemphill-Haley, 1997; Atwater and others, 2003). These sites (including Grays Harbor and the Columbia River) have a paleoseismic record spanning ~3,500 years that reveals seven probable earthquake events (Atwater and others, 2003); the turbidite record for the same interval and same region offshore includes eight events. The difference is that marine event T2 apparently was not observed at Willapa Bay (or many coastal sites). By comparison, virtually all onshore and offshore sites recorded the A.D. 1700 earthquake, with a tight grouping of dates spanning the margin. The smaller T2 event may have been recorded at Discovery Bay and other land sites (fig. 52); thus we suspect that T2 is simply below a recording or preservation threshold at some land sites.

We would expect to find less age scatter among the later, higher precision studies, and although the error ranges are smaller, there remains considerable scatter among even the best quality dates. For example, event T3, a marginwide event in the turbidite record, is well dated, with an average age of 810 ± 115 cal yr B.P. in the marine record and an average age of 860 ± 100 cal yr B.P. for the most likely correlative onshore event. However, two dates at Willapa Bay and the Salmon River skew the average age older. The age of the likely correlative event (“W”) is given as 980 ± 200 cal yr B.P. by Atwater and others (2004) at Willapa Bay, more than 100 years older than the onshore average and 150 years older than the marine average. This was a single age of very low precision, however. (In appendix 1 and figure 52, we have broken out the correlated and combined dates from Atwater and others (2004), grouped them into dates collected at Willapa Bay, Grays Harbor, and Columbia River, and recombined them in OxCal. This had virtually no effect on the age means. At the Salmon River (Nelson, A.R., and others, 2004), the likely correlative event was dated as $1,040 \pm 140$ cal yr B.P., although just as at Willapa Bay, this was a single low-precision peat age. If these dates are not included, the onshore average would be 800 ± 100 cal yr B.P., identical to the marine average. Nevertheless, onshore age means range from 990 to 700 cal yr B.P., nearly a 300-year spread as compared to ~120 years in the marine age record. The difference between the land and marine age ranges could be because several old dates are included in the land average or to an unmodeled marine reservoir effect if these data represent the same earthquake. The likely correlative dates for T4, T5, and T6 at Willapa Bay and Grays Harbor are very close to the marine averages; however,

the dates for likely T7 and T8 equivalents are well constrained and slightly younger than the marine dates. This ~100 year difference is seen at other sites, as well, and suggests a possible unmodeled reservoir effect in this time range that is applicable marginwide (as opposed to just the southern Cascadia region).

Bradley Lake, Coquille River, and Sixes River, Southern Oregon

Bradley Lake is a coastal lake in southern Oregon that contains a tsunami record of marine sands that inundated the lake. Kelsey and others (2005) established the requirements for such inundation in detail, and they concluded that the tsunami record there was attributable to local, rather than distant, tsunami. Bradley Lake however, had an event time series for which reconciliation with the offshore record initially was problematic. Several of the tsunami sands that occur in Bradley Lake seemed to be poor temporal matches for other land paleoseismic sites and for the offshore turbidite record. For example, Bradley Lake events DE3 and DE4 occur with closely spaced reported dates at about the time of small marine event T3a at ~1,000 cal yr B.P. At the same time, there is no record in Bradley Lake of temporal correlatives of marginwide T3 and T4, which likely were much larger earthquakes. Below that, another Bradley Lake event occurs at the time of small marine event T4a, rather than at the time of the larger T4 or T5 turbidites that bracket this time. Other differences include several closely spaced pairs of events in Bradley Lake, where the most likely correlative marine turbidite is interpreted as a single event. In these cases, it is possible that the marine record would be unable to resolve closely spaced events and may be missing several small events that the Bradley Lake record resolves.

The Bradley Lake record, however, may include a systematic error, which shifts the reported dates older than the event age. This is because the Bradley Lake dates, like many onshore sites, come from detrital plant material. Unlike most other sites, the material comes from a thick post-tsunami mud deposit on the bottom of the lake that overlies the tsunami sands that were swept into the lake. The massive mud deposits likely include a range of materials swept into the lake, from live plant material to detrital material that could be hundreds to thousands of years older than the event. The multiple Bradley Lake dates reported in Kelsey and others (2005) were subjected to a χ^2 test to determine which of them were grouped and therefore represented good statistical prospects for representing the event age. Because this test was done on random plant fragments with an age range of hundreds of years for each event, the test likely did not select for the best event age but rather dates that grouped statistically. The reported dates are likely biased older than the event dates because of inclusion of old detrital material. Because material that is younger than the detrital deposit is unlikely in a lake bottom setting (Kelsey and others, 2005), we have investigated using an alternate representation of the Bradley Lake dates that makes use of the youngest age from the sample group from each disturbance event in the lake. Using the youngest valid samples is common in paleoseismic investigations, where sampling represents a maximum age for the event and where

contamination by young material is precluded or unlikely, as in the Bradley Lake samples (McAlpin, 2009; Kelsey and others, 2005). The youngest sample from a group in the massive detrital deposits should represent the age closest to the event time in the lake setting. We also recalibrated the data using IntCal04 to be consistent with the marine data. As with the marine data, we found that recalibration with IntCal04 (Reimer and others, 2004) resulted in shifts of dates of 0–80 years, but more importantly, the PDFs from recalibration were, in many cases, more distinct in terms of the probability peaks, reducing the effect of multiple peaks. Presumably this results from improvements to the calibration database.

In figure 52, we plotted the Bradley Lake data using the youngest age from each event, as described here. We find this refinement of the Bradley Lake data resolves many of the discrepancies between these data and the marine turbidite record, as well as other land data, bringing many of the shifted Bradley Lake dates into closer agreement with other paleoseismic sites. Kelsey and others (2005) also used varves and sedimentation rates to estimate event dates independently, and the results of their analysis are consistent with the radiocarbon dates. The modifications we propose here (all <200 years) are within the range of 16–20 percent error in the sedimentation-rate dates given by Kelsey and others (2005, their table DR2).

The Bradley Lake record is based on tsunami-deposited sands for 12 events and on lake-sediment disturbances (possible local turbidites?) for 4 others (Kelsey and others, 2005). The Bradley Lake record exhibits a greater number of events per unit time than nearby estuary records, including 12 events that require a tsunami height of >5.5 m to reach the lake (Kelsey and others, 2005). The Bradley Lake tsunami stratigraphy includes maximum (960 yr) and minimum (22 yr) repeat times (Kelsey and others, 2005), comparable to the offshore minimum and maximum intervals of 1,190 years and 40 years, respectively).

Bradley Lake may be one of the few onshore sites that has evidence of the smaller class of earthquakes inferred at Rogue Apron, Hydrate Ridge, and other southern Cascadia offshore sites. The mean Bradley Lake recurrence interval is 390 years (<4,600 cal yr B.P.; Kelsey and others, 2005), considerably shorter than other onshore paleoseismic localities and somewhat higher than the offshore average of 220 years for 20 turbidites during the same ~4,600-year period that Bradley Lake was a good paleoseismic recorder (T1–T9a). Bradley Lake appears to be missing T2, as are other land sites, and likely is missing several of the smaller events represented in Rogue Apron cores. The temporal record at Bradley Lake exhibits clusters of events and large time gaps similar to those evident in the offshore record. For the time between T3 and T5 (~1,550–800 cal yr B.P.), the offshore record contains five turbidites and Bradley Lake includes the same number of tsunami sands. For this period, both records have a recurrence interval of ~190 years. From T5 to T6 time (~2,550–1,550 cal yr B.P.), onshore and offshore records include major events bounding this time. The offshore record also includes three very small mud turbidites, T5a, T5b, and T5c, representing events not recorded at any onshore paleoseismic site (with the possible exception of one of these recorded at the Coquille

River ~2,100 cal yr B.P.; appendix 11). Bradley Lake recorded no disturbance events during that ~1,000-year gap, which is a key link between Bradley Lake and the Rogue Apron and Hydrate Ridge sites, as well as the rest of the offshore sites, which all record this 1,000-year gap in large ruptures.

For the period from T6 to T10 time (~4,900–2,550 cal yr B.P.), the offshore record includes 11 events with a recurrence interval of 235 years, and Bradley Lake includes 8 events, with a recurrence interval of 335 years. Before that time, another large gap of ~1,000 years separates T10 and T11, a gap recorded at all marine sites. At Rogue Apron and Hydrate Ridge, this gap, like the T5–T6 gap, includes five small mud turbidites (T10a, T10b, T10c, T10d, and T10f). During this time, Bradley Lake recorded only one event, at ~5,460 cal yr B.P. The Coquille and Sixes River sites also recorded only one event during this time, with congruent dates of ~5,200 cal yr B.P. This time corresponds to the time of T10b, the largest of the small offshore turbidites. Kelsey and others (2005) attributed the lack of events during this 1,000-year period to Bradley Lake being a poor recorder during that time owing to sea-level considerations. We suggest that the reason for poor recording was the lack of large earthquakes during that period. Bradley Lake includes two older events from ~7,180 to 6,400 cal yr B.P., during which time the offshore record also includes only two large events (T11 and T13) and two very small mud turbidites (T12 and T12a).

Based on the temporal record alone, the offshore record includes 15 significant events from 7,200 to 250 cal yr B.P. (including T10b and T10f). The Bradley Lake record includes 17 events in the same period, with good temporal correspondence to the offshore data. Bradley Lake appears to be an excellent match for the offshore record, although it appears to be somewhat less sensitive to minimum earthquake size than the offshore turbidite record, but much more sensitive than other land sites. With the exception of T2, which is the smallest of the sandy turbidites, the differences between the Rogue Apron and Bradley Lake record is attributable to some of the thin mud turbidites offshore being not represented in Bradley Lake. Bradley Lake appears to include equivalents of small turbidites T3a, T4a, T7a, T8b, and T9a, providing an independent line of evidence for additional smaller earthquakes in southern Cascadia (appendix 11).

To evaluate the comparison between Rogue Apron and Bradley Lake, we compared the thickness, areal extent, and other proxies for the size and energy of the Bradley Lake disturbance events with the offshore turbidites. On the basis of the thickness and distribution of tsunami sands in Bradley Lake, Kelsey and others (2005) interpret the largest tsunamis to have been their events DE5 and DE6, which are among the largest offshore events in the same time period at Rogue Apron, suggesting a closer look. Appendix 11 shows our comparisons of event size and timing for Bradley Lake, Coquille River, and the Sixes River as compared to Rogue Apron. Although such comparisons are subject to a variety of confounding circumstances, such as the state of the tide at the time of each earthquake and the potentially complex generation of tsunami waves, we find a good correspondence between the relative size and energy of events offshore and their temporal counterparts at Bradley Lake. Small events offshore are good temporal and size matches for smaller events onshore, or are not

recorded, suggesting a threshold in recording ability at the onshore sites.

The Sixes Estuary and Coquille River onshore paleoseismic records represent the best onshore sites in southern Cascadia. The recorded events are paleoseismic events because multiple soils buried by estuary muds show evidence of coseismic subsidence, incursion of tsunami sands with marine diatoms over the wetland soil surface, and some associated liquefaction features (Atwater and Hemphill-Haley, 1997; Kelsey and others, 1998, 2000, 2002; Witter and others, 2003; Witter and Kelsey, 2004).

The Coquille River site, near Bandon, Oregon, has evidence of 12 earthquake events, all of which have been dated (Witter and others, 2003). The Coquille River site, like Bradley Lake, compares well in its temporal sequence when compared to the offshore series of larger events. From 6,600 to 250 cal yr B.P., only T3, T6, and T11 appear to be absent. Of the smaller events, the Coquille site may have equivalents of T5b, T8b, T9a, and T10b, having recorded a number of events that are likely not present marginwide, as did Bradley Lake.

The Sixes River estuary site, in Oregon, has evidence of 11 earthquake events (9 of which have been dated; Kelsey and others, 2002) in the past ~5,900 years, with a recurrence interval of ~515 years. The Sixes River paleoseismic record has a long gap, with evidence of only one undated earthquake between the A.D. 1700 earthquake and the next youngest earthquake dated at 2,000 cal yr B.P. By comparison, the offshore record includes eight earthquakes during that period: T2–T5a. Earlier than ~2,000 cal yr B.P., the Coquille River site record tracks the offshore paleoseismic record fairly well, with possible temporal correlatives for T5b, T6, T7, T8, T8a, T9, T10, T10b, and T11 (fig. 52), which, if correct, would leave T10c, T6a, T7a, T8a, T9a, T10a, and T10c–T10f unrecorded onshore. With the exception of T10f, all the missing events are of the smallest class of turbidites offshore.

The comparison of size characteristics of these two sites to the offshore record is given in appendix 11. Like Bradley Lake, the Coquille and Sixes sites track the size characteristics moderately well, with large events recorded, very small events missing, and moderate events matching up in many instances. Significant mismatches in relative size and energy proxies between onshore and offshore data were uncommon.

Saanich and Effingham Inlets, Western Vancouver Island

Several investigators have begun analyses of the recurrence pattern of turbidites along the Canadian Cascadia margin in Vancouver Island inlets and fjords. Cores in these mostly anoxic settings contain annually laminated sediments and include variable disturbances, possibly related to paleoseismic events (Dallimore and others, 2005a,b; Skinner and Bornhold, 2003; Blais-Stevens and Clague, 2001; Blais-Stevens and others, 2011). These sediment records are excellent geochronological archives of sediment-disturbance events, in some cases providing annual event-timing resolution when tied to known volcanic deposits, such as the Mazama-ash datum. The varying thickness of diatom/terrigenous mud varves in sediment cores from these anoxic basins can be interpreted in terms of annual changes in surface productivity and freshwater input within the inlet. Similarly, the occurrence

of unlaminated mud units (homogenites) intercalated amongst the laminated sediments can be interpreted in terms of oceanic and climatic changes (Dallimore and others, 2005b, 2008; Hay and others, 2009; Chang and Patterson, 2005; Chang and others, 2003). However, the sedimentary record also contains massive and graded mud units believed to arise from debris flows and turbidity currents. Some of these units probably were initiated by seismic events (seismites) corresponding to crustal and plate boundary earthquakes. These units have organic properties with a strong terrestrial signature, as opposed to other mud units in the cores that have marine affinities (Hay and others, 2009).

A large (50 cm) unit has been found in the most recent sediments of Effingham Inlet (giant Calypso core MD02-2494; Dallimore and others, 2009), as well as in other inlets farther to the north on the central mainland British Columbia coast. This deposit has been correlated to the large (magnitude 7.3) central Vancouver Island earthquake that occurred on June 23, 1946 (Dallimore and others, 2005b, 2008; Hay and others, 2009). Liquefaction of sediments, resulting in significant terrestrial and submarine slumps and slides, was initiated on both coasts of Vancouver Island by the seismic shaking associated with this earthquake, which was one of the most damaging in British Columbia's history (Rogers, 1980). This regionally recognized event bed provides a rare modern analogue for the nature of coastal marine-sediment disturbance resulting from large ($M_w \sim 7$) earthquakes and, hence, provides a proxy for the identification of other large earthquakes expressed in the sediment record.

Other paleoseismic events from the Effingham inner-basin core are interpreted as such because, like the 1946 deposit, they have wall-rock signatures from the surrounding highlands and because they show characteristics more closely resembling true turbidites than other disturbance events attributed to climate events in the cores. The deposit from the 1946 earthquake is, while much larger than the other events because of its very local source, similar in character to the events suggested as Cascadia great earthquakes (Dallimore and others, 2005b, 2008).

Similarly, cores collected in Saanich Inlet, on the eastern side of Vancouver Island, reveal a remarkably similar record of debris-flow events interspersed with varved sedimentation (Blais-Stevens and Clague, 2001; Blais-Stevens and others, 2011). Cores from ODP leg 169S and older cores established a record of synchronous deposition of debris-flow deposits at sites separated by several kilometers. Figure 52 includes the interpreted records of debris flows from Effingham and Saanich Inlets. Both records show potentially good correspondence to the marine-turbidite record and land-paleoseismic events. Saanich and Effingham cores both have potential time correlatives for a number of plate boundary earthquakes recorded by onshore and offshore paleoseismic data during the Holocene, except T8, T13, and T14, which may be represented at Saanich but not at Effingham. Events T15, T16, T17, and T18 may be present at Effingham, but data are not available for Saanich. There are a greater number of debris-flow events in Saanich Inlet than are present in the land or marine paleoseismic records for northern Cascadia. In addition to the likely correlatives, a number of other events are interspersed in the record. These events generally are thinner deposits, suggesting smaller

earthquakes or nonseismic sources. Given the known record of at least one debris-flow deposit attributable to a crustal earthquake, it is reasonable to assume that many of the smaller events originate from crustal earthquake sources, though this remains unknown at present. The recurrence intervals for all events in Saanich Inlet (1946 excepted) is very similar to that of southern Cascadia, averaging ~ 290 years for 24 events between our T13 at $\sim 7,100$ cal yr B.P. and A.D. 1700, as compared to 240 years for all events at Rogue Apron. The frequency of events capable of generating debris flows in Saanich Inlet is similar to all recorded seismic events in southern Cascadia.

As an alternative correlation test of the Effingham seismites record, we compared the physical property records of 11 candidate turbidites interpreted as Cascadia earthquakes to possible correlatives in offshore turbidite records. (Data from the upper four turbidites have not been collected because this section is a "freeze core" which cannot be removed from its storage freezer, creating some difficulties for making magnetic measurements). Six of these comparisons are shown in figure 53, which includes magnetic and density traces and radiocarbon dates for Effingham and Cascadia Channel turbidites. A strong stratigraphic physical-property signature common to both onshore and offshore cores is apparent, as is an approximate compatibility between ^{14}C dates for events T5, T6, T7, and T16 and corresponding Effingham ages. For events T10 and T11, the Effingham ages are considerably older. Four other potential correlatives have rather generic turbidite signatures that are not diagnostic, though all are compatible in age. One event is a poor radiocarbon and stratigraphic match. Dated material from the Effingham core is plant and wood material and likely represents maximum limiting ages for these events. In all but one instance (T6), the Effingham ages are older than the offshore turbidite ages.

Although many turbidites are similar, and some parameters may be somewhat autocorrelated by their fining-upward nature, several independent characteristics of the offshore deposits also are evident in the Effingham deposits. Event T5, which appears in some cores with an unusual stacking of sand units, has a density and magnetic signature that appear inverted from the normally declining-upward density and MS pattern. The Effingham signature for the potentially correlative event has a similar inverted appearance (fig. 53). The pattern of turbidite thickness for Effingham is also similar to Cascadia Channel, with events 11 and 16 being large, multipulse events in both sequences; event 10 is a small single pulse event in both sequences, and events 5, 6, 7, and 9 are moderately sized 2- or 3-pulse events in both sequences. We suggest that this evidence lends significant support to an earthquake "signature" as the common link between the onshore and offshore cores, further explored in a subsequent section. This preliminary comparison will require further study.

The record at Effingham inlet is important for advancing understanding of the Cascadia earthquake and tsunami record. At present, the coastal and marine records have much in common; however, head-to-head comparisons between onshore and marine radiocarbon dates are hindered by several issues, including reservoir correction for marine dates. The Effingham turbidites have been dated using terrestrial materials, yielding onshore dates directly comparable to onshore dates elsewhere in Cascadia,

and potentially helping to bridge the onshore-offshore gap. The stratigraphic physical-property fingerprints at Effingham may also represent an important “missing link” between the northern Cascadia onshore and offshore paleoseismic records.

Constrained Time Series

Figure 54A shows the OxCal-constrained time series for all 41 correlated events along the Cascadia margin, with segmentation indicated by symbology. These events are shown as PDFs, constrained with the Combine function in OxCal. The 2σ limits generally are narrower than shown in figure 52 owing to the Bayesian combination of multiple PDFs for events linked

by stratigraphic correlation. The events used in each combine operation are those averaged in appendix 1 (Land-Marine Compilation), and they are used elsewhere in this report where averaged regional event dates are employed for recurrence and other calculations. OxCal model inputs and outputs are given in appendixes 8 and 9. Segment D PDFs also include hemipelagic dates for events not radiocarbon dated. These computed PDFs use the Date function of OxCal inputting the calculated hemipelagic age data. The 2σ limits are generally narrower than shown in figure 52, although the simulated dates have rather broad 2σ ranges. These PDFs do not include constraints available from interevent hemipelagic intervals. Figure 54B shows the past ~7,000 years of record from the turbidite time series, compared

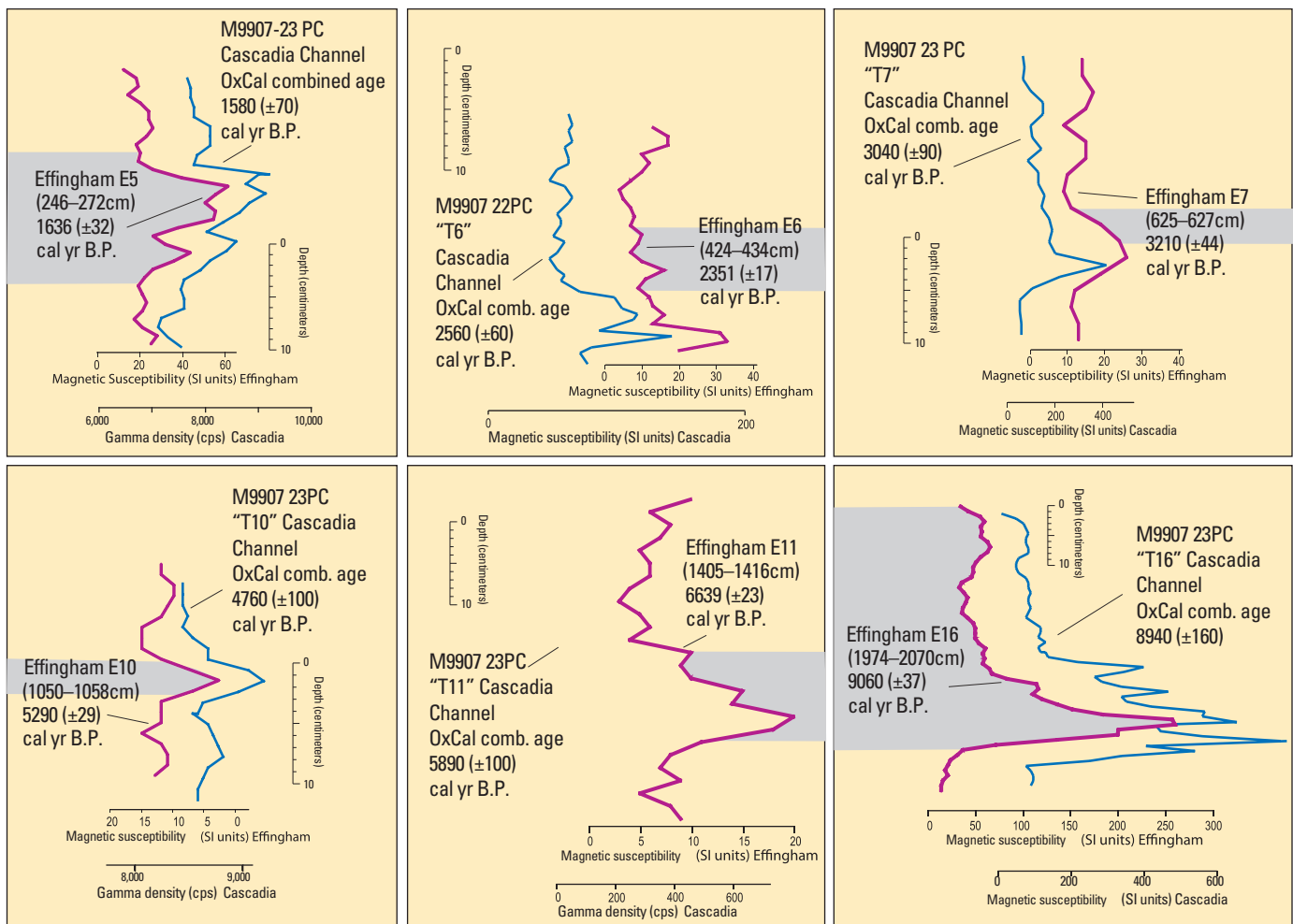


Figure 53. Preliminary correlations between Cascadia Channel core M9907-23PC and core MD02-2494 from Effingham Inlet, western Vancouver Island, Canada (see fig. 2 for core locations). Each plot shows the magnetic-susceptibility record (blue) from an Effingham Inlet (inner basin) turbidite, and a magnetic-susceptibility or gamma-density record from our 1999 cores in Cascadia Channel (purple). These events were interpreted as seismites by Dallimore and others (2005b), on the basis of wall-rock signature from the adjacent fiord walls (gray) and by comparison to the historical turbidite triggered by the 1946 Vancouver Island earthquake. The records show a striking similarity in general size, number of sandy pulses (magnetic and density peaks), and, in some cases, detailed trends. Radiocarbon ages also are first-order compatible but have separations of 100–200 years in some cases. Offshore ages are the OxCal combined ages in appendix 8 with 2σ ranges. The combined age data and stratigraphic correlation suggest that the Effingham turbidites and the Cascadia Basin turbidite signatures are recording the same earthquakes. Effingham data from Dallimore and others (2009). Abbreviations: cps, counts per second; SI, Systeme Internationale.

to the depositional history of each turbidite (Goldfinger and others 2007a, 2008). In the case of a subduction zone such as Cascadia, the source may last 3–6 minutes and may consist of multiple rupture patches, linked together but separated in time by several minutes (for example, the 2004 Sumatra earthquake; Chlieh and others, 2007). Rupture of these source patches imparts a waxing and waning shaking signal to the canyon systems and may result in multiple turbidity currents initiated within minutes of each other traveling the canyon-channel system to depocenters in the distal channels (fig. 64).

We suggest that a complex source may explain why the northern Cascadia turbidites not only pass the confluence test in number of events deposited above the Mazama ash (fig. 13), but also in stratigraphic detail, resulting in similar depositional sequences within individual turbidites in tributaries and downstream. It also can potentially explain the observed relation between Effingham Inlet magnetic signatures and our offshore cores, as well as recently observed similar linkages to southern Cascadia lakes (Morey and others, 2011). Generally, turbidite beds are observed to be more complex in proximal settings and less so in distal ones (Kneller and McCaffrey, 2003; Shiki and others, 2000b). We observe similar downstream merging and simplification of northern San Andreas Fault turbidite beds (Goldfinger and others, 2007a) and, to a lesser extent, in Cascadia. Despite this trend, the multiple fining-upward sequences are preserved over transport distances exceeding 400 km in Cascadia Basin, indicating that these are primary features of the longitudinal flow that are modified during transport by flow variability and other factors.

This may be a controversial interpretation, but we are led to it out of a need to explain the observed data. This topic is the focus of a current study involving the northern San Andreas Fault, Sumatra and Cascadia turbidites, and continuing experimental work (Garrett and others, 2011).

Time Resolution

If turbidites that have passed other tests of earthquake origin can be thought of as recorders of earthquake-source details, what sort of time resolution might they have? The question is important whether or not the origin is earthquakes because the multiple fining-upward sequences could result from earthquakes closely spaced in time, retrogressive failures over days, or other complexities. In a general way, the time represented from the base of the turbidite to the base of the fine tail that represents postevent settling of the fine clay fraction should be proportional to the source time of the initiating event(s). Given the minor differences between deposits from Juan de Fuca Channel to Cascadia Channel, a distance of 480 km, we suggest that modification by hydrodynamic processes is probably not of primary significance.

Although we cannot know precisely the amount of time required for deposition of the coarse fraction of the Cascadia turbidites, we observe that, between the fining-upward pulses, it is rare to find mud particles at the tops of the individual units. The finest material usually is fine sand and silt. Not until the uppermost sand/silt pulse is deposited do we observe the final sequence of

fining-upward mud typical of a waning turbidity current. As the current passes a fixed site, the time frame for deposition is roughly minutes to hours for deposition of coarse fractions. The short time requirement imposed by the lack of clay particles between coarse pulses implies that a series of mainshock-aftershock inputs from multiple earthquakes, or failures spread over hours to days, is not favored as a source event series. The aftershock sequence would have to take place over a span of minutes after the mainshock, which is uncommon for major aftershocks. Other explanations would be spread over even longer periods, and require mud deposition between them. A source comprising a series of rupture patches is a better fit to the observed stratigraphy, implied time constraints, and minimum magnitudes previously discussed.

Our observations of Cascadia and northern San Andreas Fault turbidites suggest that it may be possible to resolve details of seismic energy inputs that take place during a span of several minutes typical of the M_w 8–9 earthquakes known to occur in the Cascadia and San Andreas systems. If correct, interpretation of paleorupture patterns may be possible from a dense set of paleoseismic records in marine and lacustrine systems.

Conclusions

Cascadia Basin contains a variety of types and scales of turbidite systems on the continental margin from Vancouver Island, Canada, to Cape Mendocino, Calif., United States. These systems include multiple canyon sources on the Washington margin that funnel turbidites into Cascadia Channel (1,000 km length): Astoria Canyon, on the northern Oregon margin, that feeds Astoria Fan (300 km diameter) containing channel splays with depositional lobes; Rogue, Smith, and Klamath Aprons, on the southern Oregon and northern California margins, that feed small (<5 km) base-of-slope aprons; and Trinidad, Eel, and Mendocino Canyons (30–100 km length) on the northern California margin that feed into plunge pools, sediment-wave fields, and channels.

Cascadia Basin turbidite systems are an ideal place to develop a turbidite paleoseismologic method and record, because (1) a single Cascadia subduction-zone fault underlies the margin; (2) multiple tributary canyons and a variety of turbidite systems and sedimentary sources and basins exist to test for synchronous triggering of turbidity currents; (3) the presence of an excellent Mazama-ash marker provides a stratigraphic anchor in the northern two thirds of the basin; (4) during highstands of sea level, Cascadia margin physiography exerts a strong control on sediment input to canyon heads, limiting most storm/river input, except for those localities with narrow shelves; and (5) the Cascadia trench is filled, thus channel systems flow away from the margin, remaining isolated rather than merging in the trench. Detailed swath bathymetric data and core sampling procedures verify that key turbidite-channel pathways of Cascadia Basin are open and provide a good turbidite-event record. Proximal canyon-mouth and inner-fan channel areas have erratic turbidite-event records because of extensive cut-and-fill episodes in turbidity currents; however, even in these difficult locations, complete records can be found in some point bars, terraces, and canyon walls that are slightly elevated

above the channel thalweg. The most consistent turbidite event records occur in distal locations of continuous deep-sea channel systems, such as Cascadia Channel.

The similarity of the turbidite time series and good stratigraphic correlation of the turbidite event record along the northern two thirds of the Cascadia subduction zone is best explained by paleoseismic triggering of great earthquakes. Turbidites in this region pass several tests of synchronous triggering, including the “confluence test” that requires passage of multiple-source turbidites past a channel confluence in a span of a few hours, 19 consecutive times during the Holocene. Stratigraphic correlation of individual event signatures, correlation of series characteristics, such as mass and number of coarse-fraction pulses, as well as ^{14}C dates, further support synchronous triggering. Sediment supply to canyon sources appears not to be a significant controlling factor in the Holocene, partly because highstand deposition is concentrated on the shelf, and because strong ground shaking probably is sufficient to overcome variability in sediment input to the canyons.

The mismatch between the turbidite record and the frequency of teletsunami and local storms, as well as the good match in frequency and dates with earthquake and tsunami evidence onshore, also support the conclusion that the Holocene Cascadia-turbidite record primarily records earthquakes. The lack of turbidites overlying the most recent turbidite, dated to within a decade of the A.D. 1700 Cascadia earthquake, indicates that no other triggering mechanism has produced an observable turbidite in the last 300 years, except in some of the northern California channels adjacent to narrow shelves. Several sites in southern Cascadia may record a mixed storm and earthquake signal in their early Holocene sections owing to a lowered sea level. The lack of turbidite triggering in Cascadia Basin by El Niño storm and flood events (1964, 1998–99), and the 1964 Alaskan earthquake tsunami suggest that storm events and tsunami, whether or not sediment is transported to canyon heads, generally do not result in correlative abyssal-plain turbidites, except where the shelf is narrow. A small number of uncorrelated turbidites may represent crustal earthquakes or other sources.

The mean AMS age of 270 (170–390) cal yr B.P. from four channel systems for the youngest turbidite event in Cascadia Channel, T1, differs by only 15–20 years from (1) the coastal paleoseismic dates that center consistently at 250 cal yr B.P. (A.D. 1700; Nelson, A.R., and others, 1995) and (2) tsunami evidence from Japan suggesting a date of January 26, 1700, for the youngest great earthquake on the Cascadia subduction zone (Satake and others, 1996, 2003). This further validates the synchronous turbidite-event record and associated high-resolution AMS radiocarbon dates as a method to provide a long-term paleoseismic record.

The temporal correspondence between the onshore and offshore paleoseismic records along the Cascadia margin is good, despite a variety of methods and lines of evidence onshore. Within the time ranges that the two records overlap, there are few significant discrepancies. The ties between onshore and offshore paleoseismic data remain limited to radiocarbon timing for most sites, but three more direct links have emerged. Effingham Inlet on Vancouver Island contains turbidites with possible stratigraphic correlatives offshore, and Bradley Lake appears to have a reasonable correlation based on event-size characteristics in addition to radiocarbon

evidence. Other lakes onshore likely also contain earthquake turbidite stratigraphy. All three links represent more direct linkages than those available through radiocarbon dating alone.

AMS radiocarbon dates downcore for individual turbidite events show that the average recurrence interval for full-margin paleoseismic events (900–1,100 km in length) is ~500–530 years, with a variance ranging from ~200 to 1,200 years. A series of smaller ruptures, represented by thinner turbidites of lesser areal extent, can be correlated among southern Cascadia cores and has moderately good correspondence with the presence of events of limited extent at coastal paleoseismic sites. These smaller events define three other margin segments that have recurrence intervals of 410–500, 300–380, and 220–240 years for segments with northern terminations at approximately lat 46° N. (Nehalem Bank), lat 44° N. (Heceta Bank), and lat 43° N. (Coquille Bank). For full-margin ruptures, the Holocene time series implies a probability during the next 50 years of 7–11 percent of a Cascadia earthquake by using either a Poisson or time-dependent calculation. Conditional probabilities for the next 50 years are similar. Using failure-analysis statistics, the Cascadia megathrust will have exceeded ~25 percent of known recurrence intervals by a target date of 2060. For the southern segment, with a recurrence of ~240 years, probability of an earthquake occurring in the next 50 years rises to 18 percent for a Poisson distribution and 32–43 percent for a time-dependent model. Failure analysis indicates that, by the year 2060, ~85 percent of recurrence intervals will have been exceeded along the southern margin. It is also highly likely that the next event will be a southern-margin event because these occur between all known pairs of longer ruptures.

We find a strong correspondence between turbidite mass among separate margin sites, suggesting that mass of the turbidites may crudely represent earthquake magnitude and shaking duration or strength. We further find a moderate correspondence between turbidite mass and the time following each event. We conclude that there is a reasonable possibility that if the turbidite mass represents a proxy for magnitude, then the central and northern Cascadia margin may weakly follow a “time-predictable” model of recurrence. The long paleoseismic record also indicates a repeating pattern of clustered earthquakes that includes four Holocene cycles of two to five earthquakes separated by unusually long intervals of 700–1,200 years. Two of the four cycles terminated with what were likely very large earthquakes. We suggest that the good correlation of stratigraphic details along strike for many individual beds implies a common source, which may be the heterogeneity of the rupture of the initiating earthquake.

We find that the pattern of long recurrence intervals and long ruptures along the northern and central Cascadia margin is consistent with the thick sediment supply along that part of the margin. Where sediment supply thins along the southern margin, recurrence intervals and rupture lengths shorten, consistent with a model of greater interaction between lower plate and forearc structures in those areas, providing barriers to rupture propagation as well as points of nucleation not present along most of the northern margin.

Finally, Cascadia Basin investigations establish new paleoseismic techniques using marine-turbidite event stratigraphy during sea-level highstands. These investigations can be applied

in other specific settings worldwide, where an extensive fault traverses a continental margin that has several active turbidite systems and favorable physiography.

Lessons Learned

An important consideration for investigations using turbidites to develop a paleoseismic record along a major submarine fault system is an adequate number of samples and good areal coverage. In the case of Cascadia, the sample cruise was 30 sea days, and more than 102 new cores were used, along with ~60 older cores. A similar number of cores were collected for the San Andreas work (Goldfinger and others, 2007a) and the Sumatra work that is just getting underway (Patton and others, 2009). During the analysis of these data, we began with cores and locations that were well known from previous work and, therefore, had some of the details worked out. Over time, as we gained confidence in the methods, we extended the analysis to more difficult sites, finally working with cores that we initially had rejected as not being useful for turbidite stratigraphy and (or) paleoseismology. We learned, by studying the cores, which sites made good recorders of earthquakes and which did not. This led to a better understanding of the sensitivity of each site to the earthquake record: some sites being too sensitive, as evidenced by gravel lag and missing sediment section, and others with low sensitivity, as shown by thin mud turbidites and subdued log signatures. With only a few cores, we could possibly have developed a partial record: but much of the evidence for correlation, rupture lengths, and relations between time and turbidite characteristics requires broad areal sampling and replicate cores to improve the robustness of interpretations. A reduced number of samples could lead to biased or incorrect conclusions based on the biases inherent in a smaller dataset.

Blumberg and others (2008) discussed the turbidite paleoseismology of the Chile margin using two existing cores; their study may illustrate some of the issues involved with sparse data. Neither core was sited with earthquake turbidites in mind, and one ODP site was chosen as a paleoceanographic site specifically to avoid turbidites. The primary site used was on the outer trench wall, well above the trench floor, and was designed to be elevated above the influence of turbidites that would have to travel across the trench floor and central channel and up the outer trench wall to reach the site. Nevertheless, the cores from Site 1232 had more than 600 turbidites in the 64-m core, spanning ~138,000 years. During highstands, the turbidite frequency was less than one per 1,000 years, much lower than the recent onshore earthquake record. During lowstand times, the frequency increased to one every 200–300 years, similar to the earthquake record onshore. With only a single core located poorly for the purpose, we infer that the record at Site 1232 likely underestimates the number of earthquakes during all times and may include a mixed record of flood events during lowstand intervals. Without additional data from a number of sites, however, conclusions about earthquakes and climate are, at best, difficult to resolve.

Applicability to Other Settings

As we have gained experience with marine paleoseismology, we have come to realize that Cascadia is a highly favorable locality for the turbidite technique. It has a shallow plate dip and filled trench, which promote development of fan systems and discrete channel systems leading away from the margin, rather than merging on the trench floor as is more common in subduction settings. Cascadia also is in a region of upwelling and high productivity, as well as high sediment input from rivers. The hemipelagic sediment between turbidites is a mix of biogenic and extremely fine material from river plumes accumulating at a rate of ~1 m/10,000 years in Cascadia Basin. This yields just enough datable material and separation between turbidites for good stratigraphic discrimination and correlation. Cascadia Basin is mostly above the CCD, allowing good preservation of datable calcareous microfossils. Most importantly, Cascadia has large-magnitude ($M_w \sim 9?$) events at fairly regular intervals with long recurrence times, enough to allow accumulation of datable foraminifers between most events.

Few other settings have as many favorable factors, such that modification of the techniques used here is needed for most other settings. For example, the northern San Andreas Fault lies adjacent to a margin that shares many of the favorable conditions for turbidite distribution and dating that we found in Cascadia; however, the earthquake source is more distant, partly because the fault is vertical and because the shelf is wider. Earthquakes on the northern San Andreas Fault are smaller (maximum of $M_w \sim 8$, limited by crustal thickness), and the sedimentation rates are lower, factors that make the northern San Andreas Fault turbidite record more difficult to define than the Cascadia record. In Sumatra, we have started a new study to help define segments and paleoseismic recurrence along the Sumatra margin; however, many of the favorable features found in Cascadia are absent. The trench is not filled along Sumatra, the plate dip is steeper, and the trench depth ranges from 4,000 to 6,500 m, below the CCD. This means that there is no datable material in the Sumatra trench. Moreover, channels leading from the margin all merge and travel southward in the well-expressed trench. Many trench systems are more similar to Sumatra than to Cascadia, so it is worth considering alternate strategies to deal with these issues.

In Sumatra, as in Cascadia, we have found that well-selected slope basins are a good alternative. They can be selected to be above the CCD and in more productive shallower waters to increase the sedimentation rate and provide datable microfossils. With dating and stratigraphic correlation, it is possible to link sites and test for earthquake origin, although without the elegant confluence test. The trench is divided by subducting fracture zones into compartments that do not communicate with each other, somewhat relieving the problem of turbidity currents merging in the trench. This is common in the world's trenches and can be used to isolate seismic segments of the margin, which may also be controlled by subducting lower-plate structures.

Future Directions

The utility of turbidite stratigraphy has now allowed robust determination of long earthquake histories along the Cascadia margin and the northern San Andreas margin, and work is underway in Japan, along the Sumatra margin, on the southwest Iberian margin, and elsewhere. The difficulties are somewhat greater than for onshore paleoseismology, but once overcome, the rewards are significant. Because marine sedimentation is continuous, along-strike stratigraphic correlation is possible, as well as development of very long records critical to the understanding of plate-boundary processes and earthquake probabilities. At present, dating of individual events is hindered slightly by the lack of regional reservoir models for the worlds' oceans that cover time periods older than the 20th century. Such models will be needed for both paleoseismic and paleoclimatic studies and are under development in some areas.

In addition to dating past earthquakes, the correlation results presented here, and by Goldfinger and others (2007a, 2008), suggest that more information can be gleaned from the turbidites than just the dates of past earthquakes. The success of the physical-property-based correlation methods and the presence of independent "fingerprint" records in settings, such as Hydrate Ridge and Effingham Inlet, suggest that turbidites may be crude recorders of the original earthquake-rupture sequence, rather than just random sediment deposition controlled by each canyon and the hydrodynamics of transport. If this is the case, information about magnitude, rupture pattern, and perhaps directivity, may be obtained from turbidite records in the future. Testing of this hypothesis can be done in the laboratory and on deposits from the 1906 San Andreas earthquake, the 2004 and 2005 Sumatra earthquakes, the 2011 Tohoku earthquake, and other instrumental events that can be sampled in lacustrine or offshore environments. Lastly, long records may yield clues to fundamental models of earthquake recurrence based on actual occurrence over long time spans rather than inferred from short instrumental records.

Acknowledgments

We thank the investigators who have contributed to this research. Richard Boettcher analyzed and picked planktic foraminifera for radiocarbon dates. Michael Kashgarian and John Southon ran the majority of the AMS radiocarbon dates and assisted with many radiocarbon issues. Rob Wheatcroft ran ^{210}Pb samples. We acknowledge Rob Witter and Harvey Kelsey for detailed discussion of the Bradley Lake ^{14}C ages and possible modifications presented here. We also are grateful for the following students, graduate students, and their sponsoring universities, whose assistance was invaluable for the success of the 1999 and 2002 cruises: Mike Winkler, Pete Kalk, Antonio Camarero, Clara Morri, Gita Dunhill, Luis Ramos, Alex Raab, Nick Piasias, Jr., Mark Pourmanoutscheri, David Van Rooij, Lawrence Amy, Churn-Chi "Charles" Liu, Chris Moser, Devin Etheridge, Heidi Stenner, Chris Popham, Claire McKee, Duncan

McMillan, Chris Crosby, Susanne Schmid, Eulalia Gràcia, Suzanne Lovelady, Chris Romsos, Vincent Rinterknecht, Rondi Robison, David Casas, Francois Charlet, Britta Hinrichsen, Jeremiah Oxford, Miquel Marin, Marta Mas, Sergio Montes, Raquel Villalonga, Alexis Vizcaino, Santiago Jimenez, Mayte Pedrosa, Silvia Perez, Jorge Perez, Andreu Turra, David Lamas, Himar Falcon, and Andres Baranco. Captain Tom Desjardins and the officers and crews of the R/V *Melville* and R/V *Roger Revelle* provided excellent ship handling and coring logistics for the field work. The coring techniques of Pete Kalk, Chris Moser, Bob Wilson, and Chuen-Chi "Charles" Liu provided the superb piston cores that are necessary for paleoseismic analysis. We also thank Kat Crane, Suzanne Lovelady, Beth Myers, Abi Stephen, Cheryl Hummon, Trent Carmichael, Kaileen Amish, Morgan Erhardt, Jeff Beeson, Amy Garrett, and Rachel King for help with graphics, grain size, and a variety of things. We thank Linda Lamb, Crystal Barnes, and Dave Reinert at Oregon State University for the extensive copy edit on the final manuscript.

We thank the many investigators who have provided insightful conversations, advice, and suggestions during the long course of this project, including Mary Lou Zoback, Harvey Kelsey, Alan Nelson, Kerry Sieh, Rich Briggs, David Schwartz, Rob Witter, Bill McCaffrey, Peter Houghton, Russ Wynn, Takeshi Nakajima, Ken Ikehara, Brian Atwater, Kenji Satake, Tsunemasa Shiki, Keith Kelson, Keith Knudsen, Paul Spudich and many others. We thank Ivan Wong and Ram Kulkarni for insightful discussions of earthquake probabilities.

The initial funding for this study was provided by the Coastal and Marine Geology Team of the U.S. Geological Survey. The primary funding for field work and subsequent research has been provided by NSF Awards EAR 9803081, EAR-0001074, EAR-0107120, EAR-0440427, and OCE-0550843 (reservoir model development) and OCE 0850931 (2009 cruise). The U.S. Geological Survey substantially supported this study through Cooperative Agreements 6-7440-4790, 98HQAG2206, and 99HQAG0192, and the U.S. Geological Survey National Earthquake Hazard Reduction Program grants 02HQGR0019, 03HQGR0037, 06HQGR0149, and 07HQGR0064 to Goldfinger and 02HQGR0043, 03HQGR0006, and 06HQGR0020 to Nelson. The American Chemical Society awarded support to Ph.D. student Joel Johnson for core collection and analysis at Hydrate Ridge under ACS PRF 37688-AC8.

The manuscript has benefited from thoughtful reviews by Brian Atwater and David Twitchell. The authors also greatly benefited from comments and discussion at a workshop convened at Oregon State University on November 18–19, 2010, for the purpose of reviewing turbidite paleoseismic data discussed in this report. The participants in this workshop were Arthur Frankel, John Vidale, Ray Weldon, Alan Nelson, Brian Atwater, Brian Sherrod, Craig Weaver, Ned Field, Gary Carver, C. Crouse, Ivan Wong, Mark Petersen, Roland LaForge, Vicki McConnell, Tim Walsh, Ian Madin, Rob Witter, Harvey Kelsey, Paul Johnson, Larry Phillips, Ben Sheets, Joanne Bourgeois, Chesley Williams, Jake Covault, Gordon Seitz, Paul Bodin, Robert Yeats, Guillaume St-Onge, Yumei Wang, and Ray Wells.